First-Principles Calculations of Polythiophene Derivatives

First-Principles Calculations of Polythiophene Derivatives

A dissertation submitted in partial fulfillment for the degree of Doctor of Science

Patricia Lubis

1 1 2 3 1 0 2 0 1 6

Supervisor : Prof. Mineo Saito

Graduate School of Natural Science and Technology

Division of Mathematical and Physical Sciences

Kanazawa University

October 2014

Dedicated to my beloved Daddy and Mommy,
in heaven.

Psalm 23: 1 - 6
The LORD is my Shepherd, I shall not be in want.
He makes me lie down in green pastures,
He leads me beside quiet waters,
He restores my soul.
He guides me in paths of righteousness for His Name's sake.
Even though I walk through the valley of the shadow of death,
I will fear no evil, for You are with me;
Your rod and Your staff, they comfort me
You prepare a table before me in the presence of my enemies.
You anoint my head with oil; my cup overflows.
Surely goodness and love will follow me all the days of my life,
and I will dwell in the house of the LORD forever.

List of publications:

1. **Patricia Lubis** and Mineo Saito, *Band gap design of thiophene polymers based on density functional theory*, Japanese Journal of Applied Physics Vol **53**, No. 07, pp. 071602, June (2014).

KANAZAWA UNIVERSITY

Abstract

Graduate School of Natural Science and Technology
Division of Mathematical and Physical Sciences

Doctor of Science

by Patricia Lubis

Recently, conjugated polymers attracted much attention because of organic solar cells (OSCs) applications due to their flexibility, low-cost fabrication and easy processing. However, the efficiency of OSCs is still lower than that of the conventional solar cells. To increase the efficiency of OSC, the low band gap of conjugated polymer is needed. Polythiophene is one of the useful conjugated polymers. Pristine polythiophene has a quite wide band gap [2 eV], which is unfavourable with the respect to the efficiency of OSCs. Therefore, finding the low band gap of polythiophene derivatives for OSC is necessary.

Polythiophene derivatives that we study in this work are poly(3-hexylthiophene) (P3HT), poly(2-ethenylthiophene), polyisothianapthene, (PITN) and poly(2-ethenyl-3-hexylthiophene). To calculate the band gaps of these polymers, we first calculate the finite-size of oligomers. The HOMO-LUMO calculations of finite-size oligomers are conducted by using hybrid density functional theory, with B3LYP/6-31G (d,p). Next, we fitted the HOMO-LUMO energy gaps to the extrapolation scheme equation and then estimated the band gap of infinte-length polymers.

We find that the band gaps of polythiophene derivatives are in the range of 1.1 - 1.8 eV; therefore, we demonstrate that the band gaps can be controlled using suitable derivatives. The present theoretical band gap calculations are in good agreement with the band gaps of experimental values. The difference between theory and experiment is the range of 0.1 -0.2 eV.

We also clarify the mechanisms of band gap decreases in polythiophene derivatives. We conclude that the mechanism of the band gap decrease is caused by the hexyl tail effect, the weak bond alternation and the increase of delocalized of wavefunctions. Based on the mechanisms, we predict the band gap of poly(2-ethenyl-3-hexylthiophene) is 1.39 eV. This analysis gives a new insight into the band gap design of polythiophene derivatives. Therefore, further studies based on the results of present work are expected for band gap design.

Acknowledgements

First of all, I would like to express my gratitude to Prof. Mineo Saito, my kind supervisor. Thank you very much for your time and effort in evaluate and supervise this research and dissertation. Your valuable comments undoubtedly helped to improve the quality of my writing. I also give my respect to Prof. Fumiyuki Ishii, Prof. Tatsuki Oda, Prof. Shinichi Miura, and Prof. Hidemi Nagao for their kind supports and comments.

I am thankful to the Directorate General of Higher Education (DIKTI), Indonesia, and Kanazawa University, Japan, for financial support through the Joint Scholarship Program.

I give thanks to all of computational science research group members (Mr. Jianbo Lin, Mr. M.S. Alam, Ms. Miho Nishida, Mr. Kotaka, Mr. Sholihun and Mr. M. Adhib). Thank you very much for all of your supports, helps and discussions to my research. Indonesia friends, especially in Indonesia Student Association Ishikawa (PPI Ishikawa) who are always strengthen and supports me in all conditions.

The last but not least, my brothers, sisters in law and all of my families, deeply from my heart thank you very much for giving me your unconditional love and spirit through all of my days.

Contents

List of Figures

List of Tables

Chapter 1

Introduction

1.1 Background

Nowadays, explorations of conjugated polymers are extensively carried out due to the electronic and optical properties. Many potential applications of conjugated polymers are conducted, such as light emitting diode, photovoltaic devices, field-effect transistors and elecro-magnetic shielding.[1–4] Fig.1.1 shows some well-known conjugated polymers.

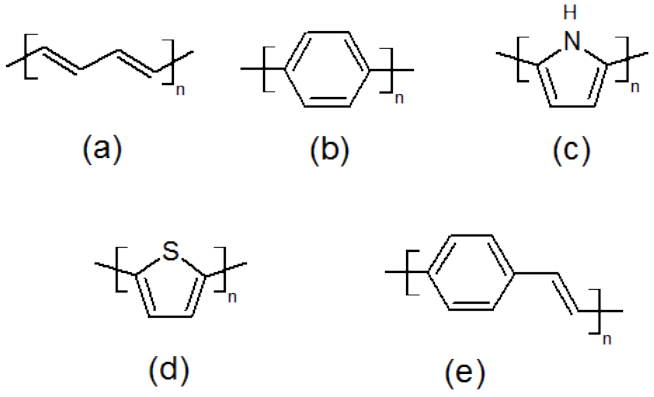

FIGURE 1.1: Some well-known conjugated polymers (a)polyacetylene, (b)polyparaphenylene, (c)polypyrole, (d)polythiophene, (e)polyparaphenylenevynilene

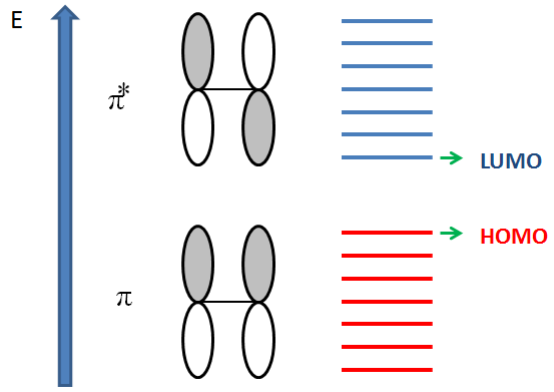

FIGURE 1.2: Bonding and antibonding illustration

Conjugated polymers consist of alternating double and single bonds of organic molecules. Conjugated polymers form sp^2 hybridized and the sp^2 bonds form three strong σ-bonds with neighbouring atoms. The remaining p_z-orbitals of the carbon atoms form delocalized electrons through the formations of weaker π-bonds. The π-electrons move from one bond to the other, which makes conjugated polymers quasi-one-dimensional semiconductors.

The π system provides delocalized electron clouds below and above the molecular plain. These π electrons play important roles in electrical and optical properties. Moreover, conjugated polymers have advantages such as, low cost fabrication, easy to synthesis, solubility.

The bands of organic semiconductors contain of highest occupied molecular orbital (HOMO) and lowest unoccupied molecular orbital (LUMO). The top of valence band corresponds to the HOMO and the lowest of conduction band correspond to the LUMO in conjugated polymers.

Conjugated polymers have useful electronic and optoelectronic properties and one of the well-known application is organic solar cells (OSCs). The development of conjugated polymers for organic solar cell (OSCs) is widely investigated. In this chapter we overview the basic of organic solar cell.

1.2 Organic Solar Cell

The idea of using organic molecules as organic photovoltaic originated from the photosynthetic systems in the early of 1950's. The plant absorbs the light and convert the solar energy into useful chemical energy. In the early experiment, the organic dyes such as phtalocyanines, chlorophylls, porphyrins were used and they are located between the anode and cathode. The efficiency of OSC is less then 1%. In 1990's, Sariciftci et al. discovered the highly efficiency organic photovoltaic by using the conjugated polymer and buckminster−fullerene (C_{60}).[5–9] Until now, the efficiency of OSC using conjugated polymer and C_{60}−like reaches 10%.[10]

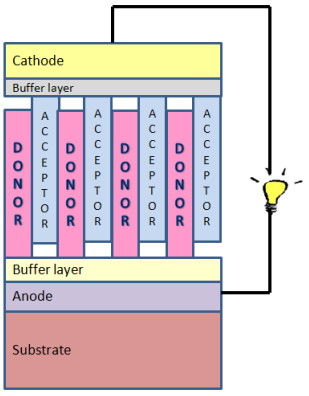

FIGURE 1.3: Organic solar cell scheme.

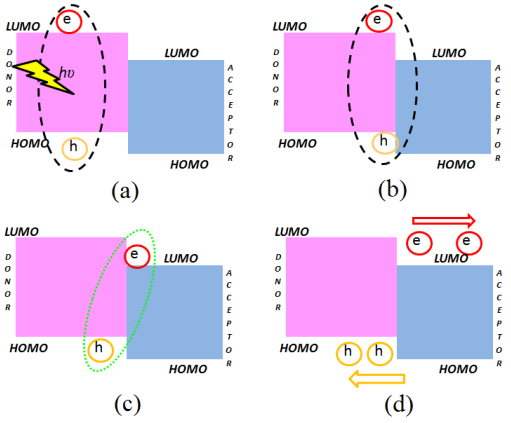

FIGURE 1.4: Organic solar cell mechanism:(a) light absorption (b) exciton diffusion (c) exciton dissociation (d) charge transfer

Organic solar cell consists of several layers, such as cathode layer, anode layer, substrate, buffer layer and an active layer. The active layer contains conjugated polymers. The active layer has function as donor and acceptor as shown in Fig.1.3. The donor (D) part produces excitons and mainly holes transport. Meanwhile the acceptor (A) part receives the electron charge.

The mechanism of photocurrents in OSC is shown in Fig.1.4.[6, 7, 9] When the photon is absorbed in the active layer especially in donor layer, the excitons are generated [Fig.1.4a]. Exciton is a bound state of an electron and a hole pair.[11, 12] The exciton is less mobile than free charges, and exhibits a small diffusion length. And then, due to the difference of concentration gradient, the excitons diffuse to donor/acceptor interface as shown in Fig.1.4(b). Next, the exciton dissociate to generate free charge carriers as shown in Fig.1.4(c). Finally, the free charge carrier is transported to the buffer layer and cathode layer, as shown in Fig.1.4(d).

The power conversion efficiency (PCE),(η) of solar cell is defined as followed,

$$\eta = \frac{P_{out}}{P_{in}} = \frac{I_{mpp} \cdot V_{mpp}}{P_{in}} = \frac{FF \cdot I_{sc} \cdot V_{oc}}{P_{in}} \tag{1.1}$$

where P_{out} is the maximum power output, P_{in} is the incident power on the solar cell. I_{sc} is short circuit photocurrent, V_{oc} is the voltage of open circuit and FF is fill factor.[6, 9] The photocurrent I_{sc} is proportional to the amount of light which is absorbed in the active layer. The absorber layer should have a wide absorption spectrum from the visible spectrum to near infra red spectrum. The V_{oc} is related to the built-in potential and V_{oc} is proportional to the difference between the energy of HOMO at the donor and the energy of the LUMO at the acceptor

$$V_{oc} \propto (1/e)(\mid E_{donor}HOMO \mid - \mid E_{acceptor}LUMO \mid) - \delta \tag{1.2}$$

where δ is the energy loss. The energy loss (δ) is associated with the possible polarization that is caused by the the exciton binding energy. Exciton is a bound electron-hole pair, the binding energy is given

$$V = \frac{e^2}{4\pi\varepsilon_r\varepsilon_0 r} \tag{1.3}$$

where ε_r is the dielectric constant of the medium, ε_0 is the permittivity vacuum, e is the charge of an electron, and r is the distance of electron-hole separation. In organic polymers, the ε_r is quite smaller ($\sim$ 3 - 4) than those of inorganic materials [ε_r silicon $\approx$ 12]. Therefore, small energy difference between the LUMO at donor the LUMO at the acceptor is required to achieve an optimum charge transfer, the energy difference is about $0.3 - 0.4eV$.[11] Then, to increase the efficiency of OSC, the short circuit photocurrent I_{sc}, open circuit voltage V_{oc} and fill factor should be maximized simultaneously. To overcome this problem, we need a low band gap of conjugated polymer; the band gap energy should be below 2 eV.[9]

1.3 The Purpose

Conjugated polymers are attractive materials for the OSC application because of the electronic, optical and mechanical properties. One of the attractive conjugated polymers is polythiophene. Polythiophene is typically a stable conjugated polymer due to aromatic structure. The advantages of polythiophene are solubility, possibility of modification and low cost fabrication. However, polythiophene has quite wide band gap, which is around 2 eV. The wide band gap of polythiophene is an obstacle to increase the OSCs efficiency. Therefore, it is necessary to find out polythiophene derivatives that have low band gaps. We studied some polythiophene derivatives as shown in Fig.1.5.

The hybrid-DFT is used to calculate the HOMO-LUMO gap energies of the finite-size oligomers. Then, we use the extrapolation scheme to predict the band gaps of infinite-length polythiophene derivatives.

We also clarify the mechanism of band gap decreases in polythiophene derivatives. The mechanism of band gap decreases can give new insight of low band gap design.

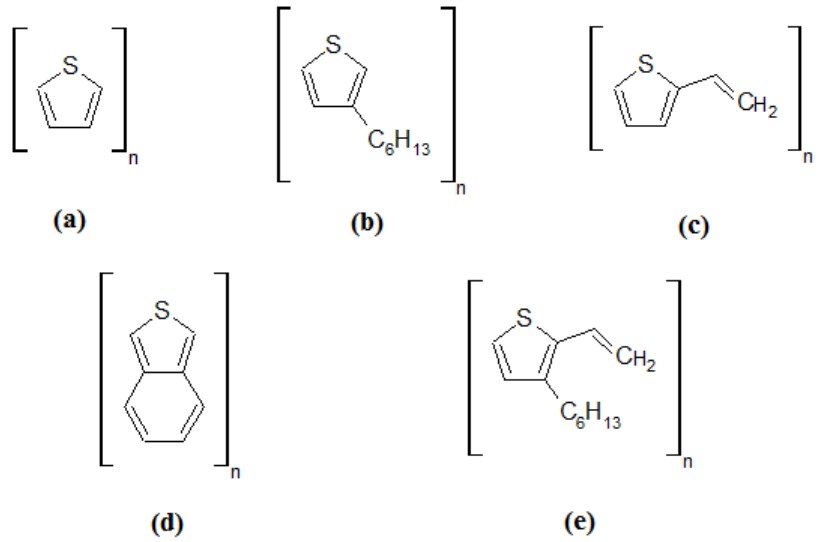

FIGURE 1.5: Thiophene derivatives: (a) Polythiophene (P1), (b) P3HT (P2), (c) Poly(2-ethenylthiophene) (P3), (d) PITN (P4), and (e) Poly(2-ethenyl-3-hexylthiophene) (P5).

1.4 Outline of Dissertation

This dissertation consists of four chapters. In chapter 1, the basic concepts and definition regarding the physical properties of organic polymer are introduced. The band gap design for organic solar cell is needed to increase the efficiency of organic solar cell. In chapter 2, we explain the fundamental concept of density functional theory. The band gap calculations of polythiophene derivates using extrapolation scheme is also explained in this chapter. The reliability of band gap calculations is confirmed in this chapter. In chapter 3, we show the calculation results of polythiophene derivatives. In this chapter, we also clarify the mechanism of band gap decreases. Finally, in chapter 4, we give a summary and explain the future scope.

Chapter 2

Theoretical Background

In this chapter, we explain the methods for calculation of the band gaps of polythiophene derivatives. First, we explain the basic concept of density functional theory and the parameters that we use in this calculation. Next, we confirm the reliability of electronic structure calculation. Finally, we explain the extrapolation scheme to calculate the band gap of infinite-size polymers.

2.1 Born-Oppenheimer Approximation

The Born-Oppenheimer approximation is used to solve Schrödinger equation for more complex systems.[13] The Schrödinger equations is express as

$$\widehat{H}_{mol}\Psi_(r_1, r_2, ...r_N) = E\Psi_(r_1, r_2, ...r_N) \tag{2.1}$$

The Hamiltonian operator consists of the kinetic energy for electrons($\widehat{T}_{el}$), the kinetic energy for the nuclei ($\widehat{T}_{nuc}$), the interaction between electron-electron ($\widehat{V}_{el-el}$), the interaction between nucleus-nucleus ($\widehat{V}_{nuc-nuc}$) and the interaction between electron nucleus ($\widehat{V}_{el-nuc}$), which is given in the form

$$\widehat{H}_{mol} = \widehat{T}_{el} + \widehat{T}_{nuc} + \widehat{V}_{el-el} + \widehat{V}_{nuc-nuc} + \widehat{V}_{el-nuc} \tag{2.2}$$

The kinetic energies are defined as

$$\widehat{T}_{el} = \sum \frac{p_j^2}{2m_e} \tag{2.3}$$

and

$$\widehat{T}_{nuc} = \sum \frac{P_j^2}{2M_j} \tag{2.4}$$

where m_e is the electron mass and M_j is the mass of the j-th nucleus, N_{nuc} is number of atoms with nuclear charges Z_{nuc}, R_n is the cartesian position and P_n is nuclear momentum. The momentum of the electron system is p_n and r_n is electron coordinate. The interaction between particles is given by

$$\widehat{V}_{el-el} = \frac{1}{2} \sum_{i \neq j} \frac{e^2}{|r_i - r_j|} \tag{2.5}$$

$$\widehat{V}_{nuc-nuc} = \frac{1}{2} \sum_{i \neq j} \frac{Z_i Z_j e^2}{|R_i - R_j|} \tag{2.6}$$

$$\widehat{V}_{el-nuc} = -\sum_{i,j} \frac{Z_j e^2}{|r_i - R_j|}, \tag{2.7}$$

The Born-Oppenheimer approximation simplifies the Schrödinger equation with the assumption that the electrons move in the electro-static field. This assumption is due to the large mass difference between electrons and nuclei. Therefore, the Hamiltonian representation is simplified as:

$$\widehat{H}(R) = \widehat{T}_{el} + \widehat{V}_{el-el} + \widehat{V}_{el-nuc}, \tag{2.8}$$

which depends on the nuclear coordinates (R).

2.2 Density Functional Theory

Based on the density functional theory (DFT) we obtain an approximate solution for the Shrodinger equation of a many-body system.[13] In a simple way, DFT helps us to to investigate the structural, magnetic and electronic properties of molecules, materials and defects. The DFT originates from statistical theory of atoms that proposed by Thomas and Fermi in 1972. The kinetic energy of system of electrons is approximated as an explicit functional of electron density. The Thomas-Fermi approach neglected exchange and correlation among the electron as shown in Eq. 2.9

$$E_T F[n] = C_1 \int d^3 r n(r)^{5/3} + \int d^3 r V_e xt(r) n(r) + C_2 \int d^3 r n(r)^{4/3} + \frac{1}{2} \int d^3 r d^3 r' \frac{n(r) n(r')}{\mid r - r' \mid} \tag{2.9}$$

2.2.1 Basis of Density Functional Theory

DFT is based on the Hohenberg-Kohn theorem in 1964. Hohenberg-Kohn theorem consists of two theorem as follow

1. In external potential of interacting particles for any system $\upsilon_{ext}(\mathbf{r})$, the potential $\upsilon_{ext}(\mathbf{r})$ is determined uniquely, except for a constant, by the ground state particle density $n_0(\mathbf{r})$

   Proof. Suppose that there were two different external potentials $\upsilon_{ext}^{(1)}(\mathbf{r})$ and $\upsilon_{ext}^{(2)}(\mathbf{r})$ which differ by more that a constant and which lead to the same ground state density $n(\mathbf{r})$. The two external potentials lead to two different Hamiltonian, $\widehat{H}^{(1)}$ and $\widehat{H}^{(2)}$, which have different ground state wavefunction,$\psi^{(1)}$ and $\psi^{(2)}$, and hypothesized to have the same ground state density $n_0(\mathbf{r})$. Since $\psi^{(2)}$ is not the ground state of $\widehat{H}^{(1)}$, it follows that

$$E^{(1)} = \left\langle \psi^{(1)} \left| \widehat{H}^{(1)} \right| \psi^{(1)} \right\rangle < \left\langle \psi^{(2)} \left| \widehat{H}^{(1)} \right| \psi^{(2)} \right\rangle \tag{2.10}$$

The strict inequality follows if the ground state is non-degenerate, which we will assume here following the arguments of Hohenberg and Kohn. The last term in Eq.(2.7) can be written

$$\begin{aligned}\left\langle \psi^{(2)} \left| \widehat{H}^{(1)} \right| \psi^{(2)} \right\rangle &= \left\langle \psi^{(2)} \left| \widehat{H}^{(2)} \right| \psi^{(2)} \right\rangle + \left\langle \psi^{(2)} \left| \widehat{H}^{(1)} - \widehat{H}^{(2)} \right| \psi^{(2)} \right\rangle \\ &= E^{(2)} + \int d^3r \left[\upsilon_{ext}^{(1)}(\mathbf{r}) - \upsilon_{ext}^{(2)}(\mathbf{r}) \right] n_0(\mathbf{r}) \end{aligned} \tag{2.11}$$

then

$$E^{(1)} < E^{(2)} + \int d^3r \left[\upsilon_{ext}^{(1)}(\mathbf{r}) - \upsilon_{ext}^{(2)}(\mathbf{r}) \right] n_0(\mathbf{r}), \tag{2.12}$$

On other hand if we consider $E^{(2)}$ in exactly the same way, we find the same equation by exchanging superscripts (1) and (2),

$$E^{(2)} < E^{(1)} + \int d^3r \left[\upsilon_{ext}^{(1)}(\mathbf{r}) - \upsilon_{ext}^{(2)}(\mathbf{r}) \right] n_0(\mathbf{r}) \tag{2.13}$$

If we add Eq.(2.9) and Eq.(2.10) we arrive at the contradictory inequality $E^{(1)} + E^{(2)} < E^{(1)} + E^{(2)}$. This provides the favor result: there cannot be two different external potentials differing by more than a constant which give rise to the same non-degenerate ground state charge density. The density uniquely resolves the external potential to within a constant.

Despite the demand of this result, it is clear from the analysis that no direction has been given to solve the problem. At this level we have achieved nothing : we are still confront with the initial problem of many interacting electrons moving in the potential due to the nuclei.

2. A universal functional for the energy $E[n]$ in terms of the density $n(r)$ can be represented, valid for any external potential $\upsilon_{ext}(\mathbf{r})$. For any particular $\upsilon_{ext}(\mathbf{r})$, the exact ground state energy of the system is the global minimum value of this functional, and the density $n(\mathbf{r})$ that minimizes the functional is the exact ground state density $n_0(\mathbf{r})$

Proof. Since all properties such as the kinetic energy, etc., are uniquely defined if $n(\mathbf{r})$ is described, then each such property can be noticed as a functional of $n(\mathbf{r})$, along with the total energy functional

$$\begin{aligned} E_{HK}[n] &= T[n] + E_{int}[n] + \int \upsilon_{ext}(\mathbf{r})\, n(\mathbf{r})\, d^3r + E_{II} \\ &= F[n] + \int \upsilon_{ext}(\mathbf{r})\, n(\mathbf{r})\, d^3r + E_{II} \end{aligned} \tag{2.14}$$

where E_{II} is the interaction energy of nuclei and $F[n]$ is a universal functional because the analysis of the kinetic and internal potential energies are the same for all systems.

Now consider a system with the ground state density $n^{(1)}(\mathbf{r})$ corresponding to external potential $\upsilon_{ext}^{(1)}(\mathbf{r})$.

$$\begin{aligned} E^{(1)} &= E_{HK}\left[n^{(1)}\right] \\ &= \left\langle \psi^{(1)} \left| \widehat{H}^{(1)} \right| \psi^{(1)} \right\rangle \end{aligned} \tag{2.15}$$

Now consider a different density, say $n^{(2)}(\mathbf{r})$, which necessarily corresponds to a different wavefunction $\psi^{(2)}$. It follows immediately that the energy $E^{(2)}$ of this state is greater that $E^{(1)}$, since

$$E^{(1)} = \left\langle \psi^{(1)} \left| \widehat{H}^{(1)} \right| \psi^{(1)} \right\rangle$$

$$< \left\langle \psi^{(2)} \left| \widehat{H}^{(1)} \right| \psi^{(2)} \right\rangle \tag{2.16}$$

$$= E^{(2)} \tag{2.17}$$

It follows that minimizing with respect to $n(\mathbf{r})$ the total energy of the system written as a functional of $n(\mathbf{r})$, one finds the total energy of the ground state. The correct density that minimizes the energy is then the ground state density

2.2.2 Kohn-Sham Equation

While the Hohenberg-Kohn theorem shows it is possible to use the ground state density to calculate properties of the system, it does not provide a way of finding the ground state density. The Kohn-Sham equations provide the framework for finding the exact density and energy of the ground state of a many-body electron problem using standard independent-particle methods.

The original expression for the Kohn-Sham energy functional is given by Eq.(2.15)

$$E\left[n\right] = T_s\left[n\right] + \int \upsilon_{ext}\left(\mathbf{r}\right) n\left(\mathbf{r}\right) d\mathbf{r} + \upsilon_H\left[n\right] + E_{xc}\left[n\right] \tag{2.18}$$

where $\upsilon_{ext}\left(\mathbf{r}\right)$ is the external potential acting on the interacting system (at minimum, for a molecular system, the electron-nuclei interaction E_{II}) the independent-particle kinetic energy $T_s\left[n\right]$ is given by

$$T_s\left[n\right] = \sum_{i=1}^{N} \psi_i^*\left(r\right) \left(-\frac{\hbar^2}{2m}\nabla^2\right) \psi_i\left(r\right) d\mathbf{r} \tag{2.19}$$

and we defined the classical Coulumb interaction energy of the electron density $n\left(\mathbf{r}\right)$ interacting with itself (the Hartree energy)

$$\upsilon_H\left[n\right] = \frac{1}{2}\int \frac{n\left(\mathbf{r}\right) n'\left(\mathbf{r}\right)}{\left|\mathbf{r}-\mathbf{r}'\right|} d^3\mathbf{r}\; d^3\mathbf{r}' \tag{2.20}$$

and $E_{xc}\left[n\right]$ is the exchange-correlation energy. It contains all the unknown contribution and is also the independent of the external potential

$$\upsilon_{xc} = \frac{\delta E_{xc}\left[n\right]}{\delta n\left(\mathbf{r}\right)} \tag{2.21}$$

We can write the Schrodinger equation for one electron system as follows

$$\left[-\frac{\hbar^2}{2m}\nabla^2 + \upsilon_{ext} + \upsilon_H + \upsilon_{xc}\right] \psi_i\left(r\right) = \varepsilon_i \psi_i\left(r\right) \tag{2.22}$$

Since the Hartree term and υ_{xc} depend on $n(\mathbf{r})$, which depend on ψ_i, the problem of solving the Kohn-Sham equation equation has to be done in a self-consistent (iterative) way. Usually one starts with an initial guess for $n(\mathbf{r})$, then calculates the corresponding υ_H and υ_{xc} and solves the Kohn-Sham equations for the ψ_i . From these one calculates a new density and starts again. This procedure is then repeated until convergence is reached

2.3 Exchange and Correlation Functional

Density functional theory is the most widely used method today for electronic structure calculations because of the success of practical, approximation functionals. The crucial quantity in the Kohn-Sham approach is the exchange-correlation energy which is expressed as a functional of the density $E_{xc}[n]$. In physics the most widely used approximation is the local-density approximation (LDA), where the functional depends only on the density at the coordinate where the functional is evaluated

$$E_{xc}^{LDA}[n] = \int \epsilon_{xc}(n)\, n(r) \quad d^3r \tag{2.23}$$

The local spin-density approximation (LSDA) is a straightforward generalization of the LDA to include electron spin:

$$E_{xc}^{LDA}[n_\uparrow, n_\downarrow] = \int \epsilon_{xc}(n_\uparrow, n_\downarrow)\, n(r) \quad d^3r \tag{2.24}$$

Highly accurate formula for the exchange-correlation energy density $\epsilon_{xc}(n_\uparrow n_\downarrow)$ has been constructed from quantum Monte Carlo simulations of Hellium. Generalized gradient approximations (GGA) are still local but also take into account the gradient of the density at the same coordinate

$$E_{xc}^{GGA}[n_\uparrow, n_\downarrow] = \int \epsilon_{xc}(n_\uparrow, n_\downarrow, \nabla n_\uparrow, \nabla n_\downarrow)\, n(r) \quad d^3r \tag{2.25}$$

Using the latter GGA is reliable results for molecular geometries and ground-state energies have been achieved.

2.4 Hybrid-DFT

Density functional theory is a successful tool to calculate electronic structure and properties of solid system. Nowadays more accurate and reliable exchange-correlation energies have been deployed. The LDA exchange-correlation energy is reliable for properties of lattice constants, bulk moduli, equilibrum geometries and vibrational frequencies.[14]. However, the LDA over estimate bond energies and cohesive energies and thus more reliable method is necessary.[15]

The GGA introduces an explicit dependence on the gradients of the density in the the exchange-correlation functionals.[16] The GGA gives improves the overbinding tendency of LDA, however it is still insufficient for the thermochemistry of molecules. Then hybrid density functional theory is necessary.

The hybrid DFT first time was introduced by Becke. In principle the method is characterized by admixture of Fock exchange energy and density functional exchange energy. One of the famous of hybrid theory is Becke three parameter Lee-Yang-Par (B3LYP) functional. The B3LYP functional firstly is introduced by Axel Becke in 1993. The functional is developed to improve the ground state description. The exchange-correlation energy is given as follows

$$a_0 E^X_{HF} + (1 - a_0)E^X_{LDA} + a_X(E^X_{GGA} - E^X_{LDA}) + (1 - a_C)E^C_{LDA} + a_C E^C_{GGA} \quad (2.26)$$

where E^X_{HF} is the Hartree-Fock exchange energy, a_0 is 0.2, a_X is 0.72 and a_C is 0.81. In the above expression E^X_{LDA} and E^C_{LDA} are the LDA exchange and correlation energies respectively. The E^X_{GGA} and E^C_{GGA} are the GGA exchange and correlation energies, respectively.[17]

2.5 Basis Set

Among many different approximation methods to solve the Schrödinger equation, one of the approximation method is basis set. Basis sets are sets of mathematical functions. John. C. Slater proposed slater type orbitals (STOs)[18],

$$\psi = a_1\phi_1 + a_2\phi_2 + ... + a_k\phi_k \tag{2.27}$$

where k is the size of basis set, $\phi_1, \phi_2, ..., \phi_k$ are the basis functions and $a_1, a_2, ..., a_k$ are the normalizations constants. The solution of the Schrödinger equation for the hydrogen atom and other one-electron ions gives atomic orbitals which are a product of a radial functions depend on the distance of the electron from the nucleus and a spherical harmonic, as shown in Table 2.1

Slater-type orbitals describe the real situation for the electron density in the valence region and beyond. However Slater-type orbitals are not good for the near nucleus region. The general expression for a basis function is given in Eq.**??**

$$\chi_{\zeta,n,l,m}(r,\theta,\varphi) = NY_{l,m}(\theta,\varphi)r^{n-1}e^{-\zeta r} \tag{2.28}$$

TABLE 2.1: Radial and angular wavefunctions of orbitals. Here, r is the radius in atomic units (1 Bohr radius = 52.9 p.m), z is the effective nuclear charge for that orbital of the atom, $e = 2.71828$, $\pi = 3.14159$, n is the principal quantum number and $\rho = (2Zr)/n$

No.	Orbital	Radial wavefunction	Angular wavefunction
1.	$1s$	$2 \times z^{3/2} \times e^{-}\rho/2$	$1 \times (\pi/4)^{1/2}$
2.	$2s$	$(\sqrt{2}/2) \times (2-\rho) \times z^{3/2} \times e^{-}\rho/2$	$1 \times (\pi/4)^{1/2}$
3.	$2p$	$(\sqrt{6}/2) \times \rho) \times z^{3/2} \times e^{-}\rho/2$	$\sqrt{3} \times (x/r)(\pi/4)^{1/2}$
4.	$3s$	$(\sqrt{3}/9) \times (6-6\rho+\rho^2) \times z^{3/2} \times e^{-}\rho/2$	$1 \times (\pi/4)^{1/2}$
5.	$3p$	$(\sqrt{6}/9) \times \rho(4-\rho) \times z^{3/2} \times e^{-}\rho/2$	$\sqrt{3} \times (x/r)(\pi/4)^{1/2}$

where N is a normalization constant and Y_{lm} is spherical harmonic function. The exponential depend on the distance between the nucleus and the electron mirror. The n, l, and m are quantum numbers, angular momentum and magnetic, respectively. STO is commonly used for atomic and diatomic systems where high accuracy is required.

In the 1950s, Frank Boys suggested a modification of wavefunction by using Gaussian type orbitals, which contain the exponetioal $e^{\beta r^2}$, rather than $e^{\alpha r}$ of STOs. GTOs consist of several combination in linear coefficient. The GTOs basis function is expressed by

$$GTO(3G) = c_1 e^{-\beta_1 r^2} + c_2 e^{-\beta_2 r^2} + c_3 e^{-\beta_3 r^2} \tag{2.29}$$

where the three values of c and β are fixed, and that number is included in the designation. The Gaussian type orbitals can be written in term of polar or cartesian coordinates

$$\begin{aligned} \chi_{\zeta,n,l,m}(r,\theta,\varphi) &= N Y_{l,m}(\theta,\varphi) r^{2n-2-l} e^{-\zeta r^2} \\ \chi_{\zeta,l_x,l_y,l_z}()x,y,z) &= N x^{l_x} y^{l_y} z^{l_z} e^{-\zeta r^2} \end{aligned} \tag{2.30}$$

where the sum of l_x, l_y and l_z determines the type of orbital. In Gaussian functions, there are six possible d-type functions with the factor x_a^2, y_a^2, z_a^2, $x_a y_a$, $x_a z_a$ and $y_a z_a$. These d-functions can be modified into five linear combinations, as $x_a y_a$, $x_a z_a$,$y_a z$, x_a^2-y_a^2, and $3z_a^2$-r_a^2 to have the same angular behaviour as the real 3d orbitals. Within the sixth possible combination x_a^2+y_a^2+z_a^2 = r_a^2 correspond to s-orbital.

In term of computational efficiency, it is important to choose number of function can be used. Basis set can be classified in to the following types.

1. *Minimal basis sets*

   In the minimal basis set, one basis function should be choose for every atomic orbital that is required to described the free atoms. For hydrogen, minimal basis set is $1s$ orbital. For carbon, the minimal basis set consists of $1s$ and $2s$ orbitals and the full set of three $2p$ orbitals. Several basis sets have been proposed for computational purpose, such as: $STO-3G, STO-4G, STO-$

$6G, STO-3G^*$ (a polarized version of STO-3G). The $STO-nG$ basis sets devised by John Pople and his groups are the most common basis set. The $STO-nG$ basis set is a minimal basis set, where each basis function is contraction of n primitive Gaussians.

2. *Pople basis sets*

   These basis set was developed by Pople and his groups to represent the split valence type.[19] The basis set is represented as $k-nlmG$ basis sets. The k represent how many Pople Gaussian Type Orbitals ($PGTOs$) are used for corresponding the core orbitals. The nlm indicate how many functions the valence orbitals are split into and how many $PGTOs$ are used for the representation. If two values (nl) are used, it indicates a split valence. The values before the Gaussian indicate the $s-$ and $p-$ functions. However in the basis set, the values after Gaussian represent the polarization functions. Several computation method using Pople basis sets are $3-21G, 6-31G, 6-31G(d,p), 6-311G, 6-311G^*$, etc.

3. *Correlation consistent basis sets*

   The correlation consistent (cc) basis sets correspond to the correlation energy of the valence electrons. These basis sets include shells of polarization (correlating) functions (d, f, g, etc) that can yield convergence of the electronic energy to the complete basis set limit. Several different sizes of cc basis sets are known by their acronyms : cc-pVDZ (correlation consistent valence double zeta), cc-pVTZ (correlation consistent valence triple zeta), cc-pVQZ (correlation consistent valence quadruple zeta), cc-pV5Z (correlation consistent valence quintuple zeta), etc.

4. *Other split valence basis set*

   The split-valence (SV) basis sets use one function for orbitals that are not in the valence shell and two functions for those in valence shell. There are several split-valence basis sets, such as SVP (split-valence polarization), DZV (double zeta valence), TZVPP (triple valence Zeta plus polarization), QZVPP (quadruple-zeta plus polarization), etc.

5. *Double,triple and quadruple zeta basis sets*
   These basis sets are multiple basis functions that correspond to each atomic orbitals. The most common is the D95 basis set of Dunning

6. *Plane wave basis sets*
   Plane wave basis sets using a finite number of plane wavefunctions. The specific cutoff energy is chosen for certain calculations.

2.6 Reliability of Electronic Structure Calculation

The reliability of band gap calculations is shown in the basis sets performance. In this work, besides the 6-31G(d,p) basis set, we also try the band gap calculations using 6-311(d,p) and cc-pVQZ basis sets. We calculate polythiophene. The hybrid-DFT is used to calculate the HOMO-LUMO gap energy of the finite-size thiophene oligomers. We find that the band gap of the infinite-length polythiophene calculated by the 6-31G(d,p) basis set is close to those calculated using the 6-311(d,p) and cc-pVQZ basis sets. The energy difference is less than 23 meV as shown in Table 2.2. Therefore, the basis set of 6-31G(d,p) is expected to be reliable.

The reliability of our calculations for the bond angle and bond length is shown in Tables 2.3 and 2.4. The bond length and bond angle, which are calculated for the 6-mer [Fig. 2.1], are close to experimental values.[20] The deviations for the bond lengths are less than 0.002 $\mathring{A}$ [Table 2.3] and those for the bond angles are less than 2^o [Table 2.4]. Therefore, the present calculation is expected to be reliable for geometries optimization.

TABLE 2.2: Calculation of the band gap of polythiophene using several basis sets.

Basis set	Band gap (eV)
6-31G (d,p)	1.92
6-311G (d,p)	2.09
cc-pVQZ	1.86
Experiment	2.00

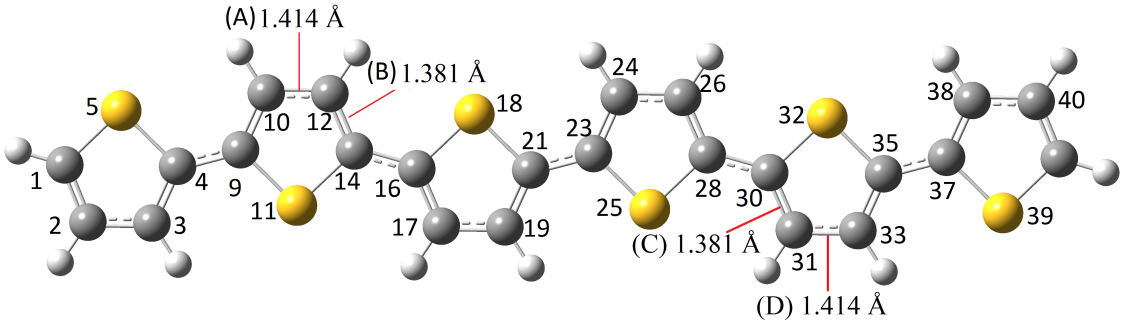

FIGURE 2.1: Molecular structure of polythiophene.

TABLE 2.3: Bond lengths of sexithiophene. Δ is the difference between calculation and experimental values. The numbers of atoms are shown in Fig. 2.1.

Bond length	Present calculation (Å)	Exp. (Å)[20]	Δ (Å)	Bond length	Present calculation (Å)	Exp. (Å)[20]	Δ (Å)
C(1)-S(5)	1.7353	1.709	0.03	C(12)-C(14)	1.3813	1.364	0.02
C(4)-S(5)	1.7581	1.730	0.03	C(14)-C(16)	1.4414	1.444	0.00
C(9)-S(11)	1.7574	1.736	0.02	C(16)-C(17)	1.3819	1.370	0.01
C(14)-S(11	1.7588	1.738	0.02	C(17)-C(19)	1.4129	1.400	0.01
C(16)-S(18)	1.7587	1.731	0.03	C(19)-C(21)	1.3820	1.380	0.00
C(21)-S(18)	1.7589	1.734	0.02	C(21)-C(23)	1.4409	1.444	0.00
C(23)-S(25)	1.7589	1.732	0.03	C(23)-C(24)	1.3820	1.367	0.01
C(28)-S(25)	1.7587	1.734	0.02	C(24)-C(26)	1.4129	1.403	0.01
C(30)-S(32)	1.7588	1.736	0.02	C(26)-C(28)	1.3819	1.376	0.01
C(35)-S(32)	1.7574	1.735	0.02	C(28)-C(30)	1.4414	1.441	0.00
C(37)-S(39)	1.7581	1.721	0.04	C(30)-C(31)	1.3813	1.370	0.01
C(42)-S(39)	1.7353	1.710	0.03	C(31)-C(33)	1.4141	1.405	0.01
C(1)-C(2)	1.3674	1.342	0.03	C(33)-C(35)	1.3802	1.377	0.00
C(2)-C(3)	1.4225	1.408	0.01	C(35)-C(37)	1.4459	1.441	0.00
C(3)-C(4)	1.3798	1.388	0.01	C(37)-C(38)	1.3798	1.402	0.02
C(4)-C(9)	1.4459	1.439	0.01	C(38)-C(40)	1.4225	1.416	0.01
C(9)-C(10)	1.3802	1.365	0.02	C(40)-C(42)	1.3674	1.346	0.02
C(10)-C(12)	1.4141	1.405	0.01				

TABLE 2.4: Bond angles of sexithiophene. Δ is the difference between calculation and experimental values. The numbers of atoms are shown in Fig. 2.1.

Bond angle	Present calculation (^{o})	Exp. [20] (^{o})	Δ (^{o})	Bond angle	Present calculation (^{o})	Exp. [20] (^{o})	Δ (^{o})
C(1)-S(5)-C(4)	91.777	92.1	0.32	S(18)-C(14)-C(19)	110.018	110.3	0.28
C(9)-S(11)-C(14)	92.148	91.9	0.25	S(18)-C(19-C(23)	120.835	120.6	0.23
C(16)-S(18)-C(216)	92.132	92.2	0.07	C(19)-C(21)-C(23)	129.147	129.1	0.05
C(23)-S(25)-C(28)	92.132	92.0	0.13	S(25)-C(23)-C(21)	120.835	120.5	0.33
C(30)-S(32)-C(35)	92.148	92.2	0.05	S(25)-C(23)-C(24)	110.065	110.5	0.43
C(37)-S(39)-C(42)	91.777	92.4	0.62	C(21)-C(23)-C(24)	129.147	129.0	0.15
S(5)-C(1)-C(2)	111.660	112.3	0.64	C(23)-C(24)-C(26)	113.909	114.0	0.09
C(1)-C(2)-C(3)	112.918	112.9	0.02	C(24)-C(26)-C(28)	113.915	112.7	1.21
C(2)-C(3)-C(4)	113.638	113.1	0.54	S(25)-C(28)-C(26)	110.029	110.8	0.77
C(3)-C(4)-C(5)	110.008	109.6	0.41	S(25)-C(28)-C(30)	120.815	120.2	0.61
S(5)-C(4)-C(6)	120.901	120.8	0.10	C(26)-C(28)-C(30)	129.156	129.0	0.16
C(3)-C(4)-C(6)	129.092	129.6	0.51	S(32)-C(30)-C(28)	120.848	120.8	0.05
S(11)-C(9)-C(4)	120.800	120.5	0.30	S(32)-C(30)-C(31)	110.004	110.3	0.30
S(11)-C(9)-C(10)	110.065	110.3	0.23	C(28)-C(30)-C(31)	129.149	129.0	0.15
C(4)-C(9)-C(10)	129.134	129.2	0.07	C(30)-C(31)-C(33)	113.868	114.0	0.13
C(9)-C(10)-C(12)	113.915	113.9	0.01	C(31)-C(33)-C(35)	113.915	113.1	0.81
C(10)-C(12)-C(14)	113.868	113.3	0.57	S(32)-C(35)-C(33)	110.065	110.5	0.43
S(11)-C(14)-C(12)	110.004	110.6	0.60	S(32)-C(35)-C(37)	120.800	121.1	0.30
S(11)-C(14)-C(16)	120.848	120.4	0.45	C(33)-C(35)-C(37)	129.134	128.4	0.73
C(12)-C(14)-C(16)	129.148	129.0	0.15	S(39)-C(37)-C(35)	120.901	120.8	0.10
S(18)-C(16)-C(14)	120.815	120.2	0.61	S(39)-C(35)-C(38)	110.008	110.4	0.39
S(18)-C(16)-C(17)	110.029	110.6	0.57	C(35)-C(37)-C(38)	129.092	128.8	0.29
C(14)-C(16)-C(17)	129.156	129.2	0.04	C(37)-C(38)-C(40)	113.638	111.6	2.04
C(16)-C(17)-C(19)	113.912	113.6	0.31	C(38)-C(40)-C(42)	112.918	113.8	0.88
C(17-C(19)-C(21)	113.909	113.3	0.61	S(39)-C(42)-C(40)	111.660	111.8	0.14

2.7 Extrapolation Scheme for Estimation of Band Gaps in Conjugated Polymers

2.7.1 Extrapolation Scheme

In this work, to calculate the band gaps of infinite-size of conjugated polymers, we use extrapolation scheme method. First, we calculate the HOMO-LUMO gap energy of finite-size oligomers of polythiophne derivatives. We use Gaussian 03 installed package program and B3LYP/6-31G(d,p) method.[21] Then, we fitted the values of HOMO-LUMO gap energy using an extrapolation scheme [23],

$$E_g(N_i) = E_g + \frac{a}{N_i}, \tag{2.31}$$

where $E_g(N_i)$ corresponds to the HOMO-LUMO gap of oligomers and N_i is the number of carbon atoms in the conjugated chain in an oligomer. a and E_g are determined by fitting to the calculated values of $E_g(N_i)$, and E_g corresponds to the band gap of the infinite-length polymer, $E_g(\infty)$.

To predict the infinite-size of HOMO energy level and LUMO energy level of conjugated polymers, we use derivation of the Eq.(2.31) and then we plot the HOMO energy and LUMO energy by the following equation

$$E_{level}(N) = b_{level} + \frac{a}{N}, \tag{2.32}$$

where E_{level} is the HOMO or LUMO energies of oligomers, and N is the number of carbon atoms in a conjugated chain. b_{level} is the HOMO energy or LUMO energy of the infinite-length polymers.

2.7.2 Evaluation of Extrapolation Scheme Estimation

We also evaluate the reliability of the the extrapolation scheme using coefficient of determination, R^2, which is given by

$$R^2 = \frac{[\sum_i (\frac{1}{N_i} - < \frac{1}{N_i} >)(E_g(N_i) - < E_g(N_i) >)]^2}{\sum_i [\frac{1}{N}_i - < \frac{1}{N_i} >]^2 \sum_i [E_g(N_i) - < E_g(N_i) >]^2}, \tag{2.33}$$

where $<>$ indicates the average over i. When the value of R^2 is close to 1, the data are well fitted to Eq. (2.31). The R^2 results will be shown in the next chapter.

Chapter 3

Band Gap Design of Thiophene Polymers

3.1 Introduction

Conjugated polymer is an attractive material for OSC application. Polythiophene is one of the conjugated polymers that has attractive electronic properties. The band gap of pristine polythiophene is 2 eV. However, to increase the efficiency of OSC, the low band gap conjugated polymer is more favorable. Therefore, finding the low band gap of conjugated polymers for OSC application is necessary.[22–27] To find low band gap of conjugated polymers, we study several polythiophene derivatives as shown in Fig.1.5. For this purpose the band gap calculation is an essential tool.

The band gap calculations consist of some steps. The molecular orbital theory calculation can be used to find the band gap for finite-size of conjugated polymer. For infinite-size of conjugated polymers, the extrapolation scheme is one of the powerful tool to predict the band gap.[3, 23, 30–33].

Here, we apply the extrapolation scheme to calculate the band gaps of some polythiophene derivatives. In addition to polythiophene (P1), for the first time, we calculate the band gaps of derivatives having hexyl bases, i.e., poly(3-hexylthiophene)

[P3HT] (P2). The band gap of poly(2-ethenylthiophene) (P3) and PITN (P4) have been studied previously, in this calculation, we make comparison of band gap values between previous calculations and present calculations. These polymers are shown in Fig. 1.5. We obtain good agreement between theoretical and experimental band gaps of P1, P2, P3, and P4. Furthermore, we predict the band gap of P5, which has not yet been determined. We find that calculated band gaps are 1.10 - 1.81 eV; therefore, we demonstrate that the band gaps can be controlled using suitable derivatives. In this chapter, we analyze the HOMO and LUMO of polythiophene and its derivatives for the first time and clarify the mechanism underlying the decreases in the band gaps of the derivatives. This analysis gives a new insight into the band gap design of polythiophene derivatives.

3.2 Results

3.2.1 Polythiophene (P1)

The band gap of infinite-size polythiophene carried out by using hybrid-DFT. The calculations from monomer until 30-mer of thiophene [Fig. 1.5(a)]. After that, we estimate the band gap of the infinite-size polymer using the extrapolation scheme. As shown in Fig. 3.1, the calculated HOMO-LUMO gaps of the oligomers are well fitted to Eq. (2.31).

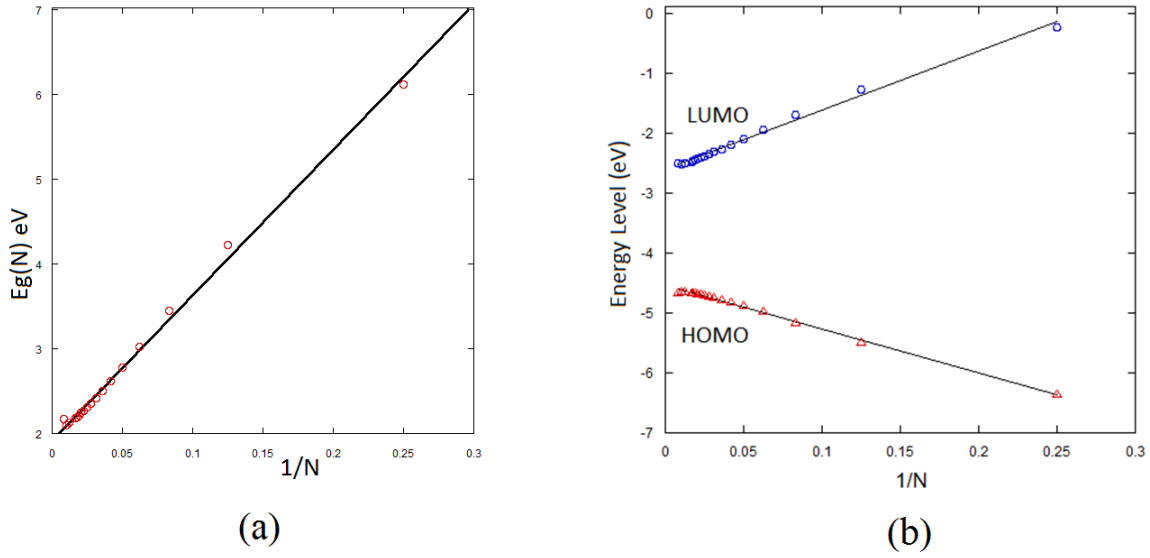

FIGURE 3.1: Calculation of P1 oligomers (a) Band gap and (b) HOMO and LUMO energy level.

The calculations of the oligomers are well fitted, since R^2 is close to 1. Therefore, we successfully determine the band gap of the infinite-size polythiophene: the estimated value is 1.92 eV [Table 3.1], which is close to the experimental value (2.0 eV)[22].

TABLE 3.1: Band gaps of polythiophene derivatives calculated using the extrapolation scheme. N_{max} is the number of carbon atoms in the conjugated chain for the maximum oligomer used in the calculations.

System	HOMO (eV)	LUMO (eV)	Eg (eV)	Eg (Exp.) (eV)	R^2	N_{max}
P1	-4.52	-2.6	1.92	2 [22]	0.9964	120
P2	-4.09	-2.28	1.81	1.8 [3]	0.9948	52
P3	-4.41	-2.80	1.61	1.8 [28]	0.9955	66
P4	-4.02	-2.92	1.10	1.1 [3]	0.9953	120
P5	-4.08	-2.69	1.39	-	0.9936	106

TABLE 3.2: Calculated HOMO-LUMO gaps of thiophene derivatives monomers.

System	HOMO (eV)	LUMO (eV)	HOMO-LUMO gap (eV)
P1	-6.35	-0.23	6.12
P2	-6.15	-0.04	6.11
P3	-5.76	-1.02	4.74
P4	-5.62	-0.89	4.73
P5	-5.39	-1.38	4.01

As shown in Fig. 3.1(b), the calculated energies of HOMO and LUMO are well fitted to Eq. (2.32). In the case of the monomer, the HOMO and LUMO energies are -6.35 and -0.23 eV, respectively; therefore, the HOMO-LUMO gap is 6.12 eV, as shown in Table 3.2. We estimate that the energies of HOMO and LUMO in the infinite-size polymer are -4.52 and -2.60 eV, respectively. Therefore, the HOMO-LUMO gap of the polymer is 4.20 eV lower than that of the monomer.

The HOMO has bonding phases for the double bonds in the conjugated chain [Fig. 3.2(a)], whereas the LUMO has bonding phases for the single bonds [Fig. 3.2(b)]. Both HOMO and LUMO consist of the carbon p orbitals, which are perpendicular to the molecular plane.

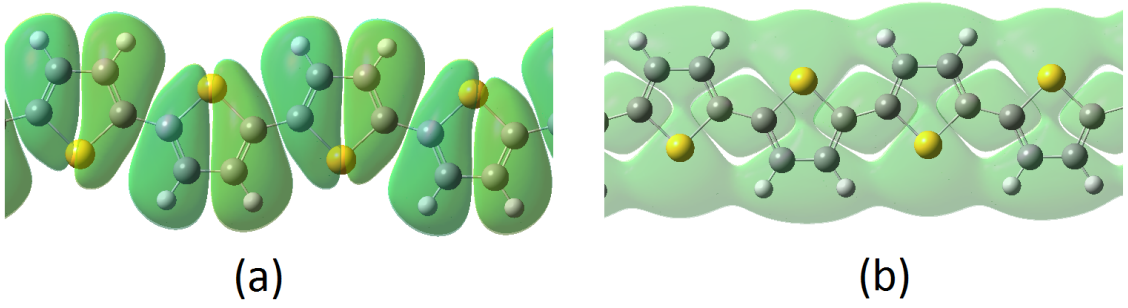

FIGURE 3.2: P1 wavefunction. The isovalue is 0.002 atomic unit: (a) HOMO wavefunction and (b) LUMO wavefunction.

In the monomer, the lengths of the double bond and single bond are 1.367 and 1.430 Å, respectively. In the 10-mer, the double-bond and single-bond lengths at the edges are 1.367 and 1.422 Å, respectively, which are close to those of the monomer. In contrast, the lengths of the double and single bonds at the center are 1.382 and 1.412 Å, respectively, as shown in Fig. 3.3. Therefore, the bond length alternation at the center in the 10-mer is weaker than in the monomer. In the case of the 30-mer, the lengths of the short bonds (1.382 Å) and long bonds (1.413 Å) at the center are close to those of the 10-mer. Therefore, we expect that these values are close to those of the infinite-length polymers. These results suggest that the bond alternation in the infinite-length polymer is expected to be weaker than that in the monomer. This weak bond alternation in the polymer is expected to contribute to the decrease in band gap compared with that in the monomer.[24, 25]

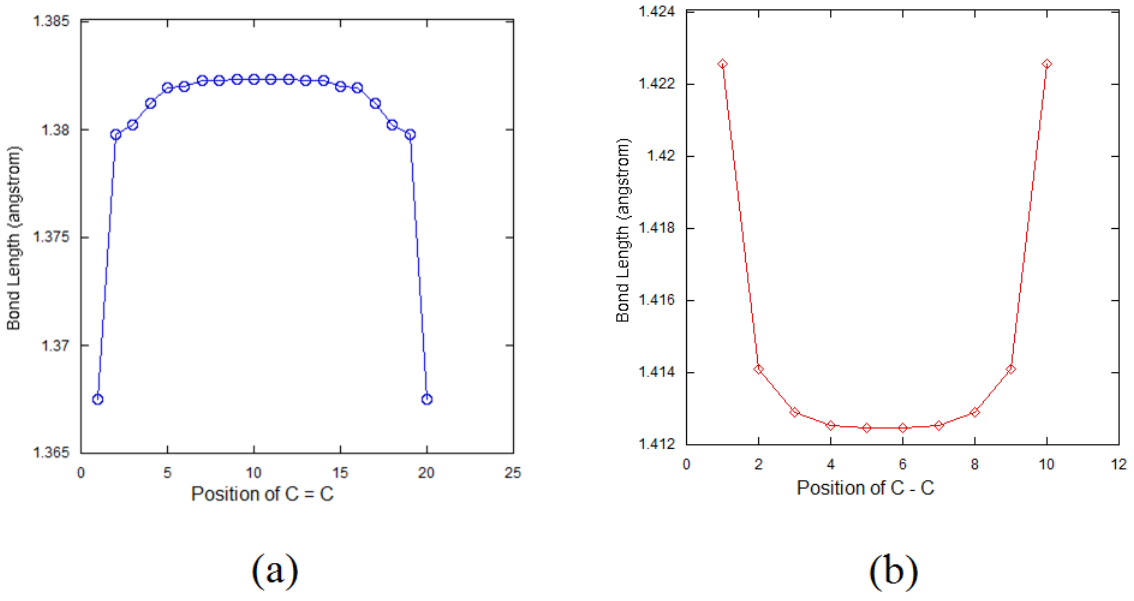

FIGURE 3.3: Bond lengths of the π bond chain in P1 10-mer: (a) Double-bond lengths in thiophene backbone from an end of the oligomer and (b) Single-bond lengths in thiophene backbone from an end of the oligomer.

3.2.2 P3HT (P2)

The band gap calculation of thiophene derivatives with alkyl based using extrapolation scheme for the first time is calculated. P2 consists of thiophene and hexyl [Fig. 1.5(b)]. We calculate P2 using hybrid-DFT from the monomer to the 13-mer. Next, the HOMO-LUMO gap energies of the P2 oligomers are fitted to the extrapolation scheme. Fig. 3.4(a) shows the HOMO-LUMO gap values are fitted well to find out the infinite band gap. The HOMO energy level and LUMO energy level of infinite-size polymer are also fitted appropriately as shown in Fig. 3.4(b).

We estimate the band gap of the infinite-size polymer to be 1.81 eV, which is close to the experimental value (1.8 eV)[3]. The band gap of P2 is 0.11 eV lower than that of P1. We estimate that the energies of HOMO and LUMO in the infinite-length polymer are -4.09 and -2.28 eV, respectively, as shown in Table 3.1.

Therefore, the energy of the HOMO of P2 is 0.43 eV higher than that of P1, and the energy of LUMO of P2 is 0.32 eV higher than that of P1. Thus, the energy increase of the HOMO is 0.11 eV larger than that of the LUMO. This is the reason why the band gap of P2 is 0.11 eV lower than that of P1.

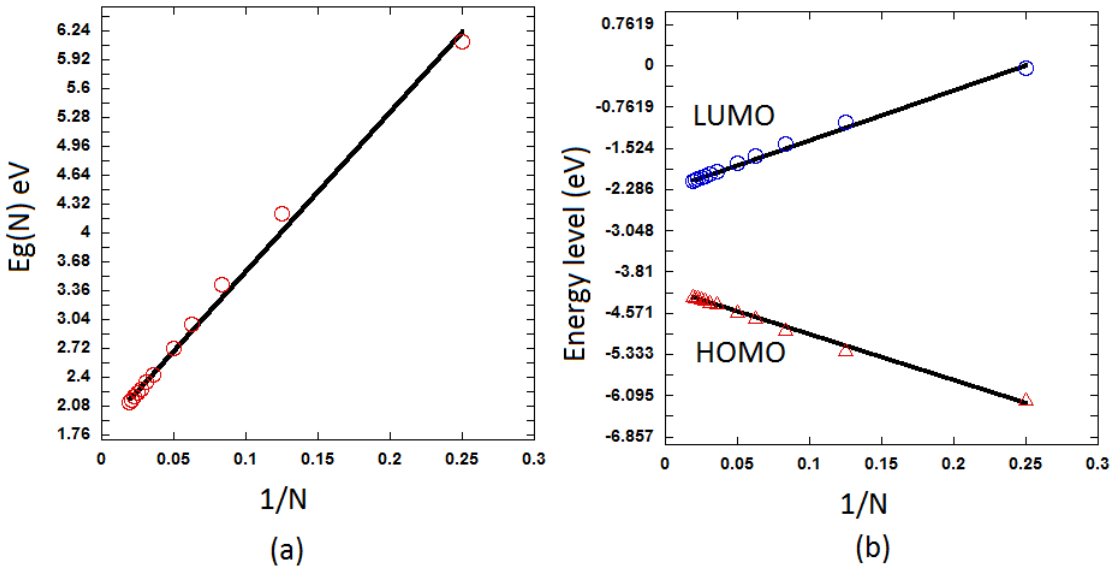

FIGURE 3.4: Calculation of P2 (a) Band gap and (b) HOMO and LUMO energy level.

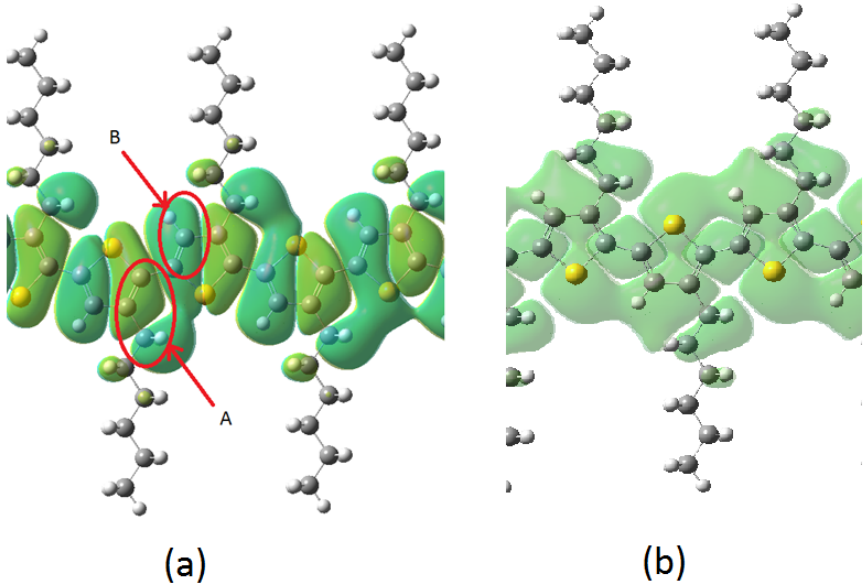

FIGURE 3.5: P2 wavefunction. The isovalue is 0.002 atomic unit: (a) HOMO wavefunction and (b) LUMO wavefunction.

The above-mentioned low band gap of this system is expected to originate from the interaction between the hexyl of the thiophene backbone [which is indicated by A in Fig. 3.5(a)] and the double bond of the thiophene backbone without the hexyl [which is indicated by B in Fig. 3.5(a)]. This interaction leads to the large increase in HOMO energy since the HOMO has the bonding phase for the double bond in the conjugated chain [Fig. 3.5(a)]. The effect of the interaction on the LUMO is weak, as Fig. 3.5(b) shows, which causes a small increase in LUMO energy.

Although the band gap of P2 is lower than that of P1, the HOMO-LUMO gap of the monomer of P2 (6.11 eV) is very similar to that of P1(6.12 eV) [Table 3.2]. This similarity in energy is due to the fact that there is no interaction between the hexyl and the double bond in P1 in the case of the monomer of P2.

The interaction between the double bond and hexyl affects the bond length. We show the results for the 10-mer in Fig. 3.6(a). We find that the lengths of the double bonds in the thiophene backbone of P2 osccilate at the center.

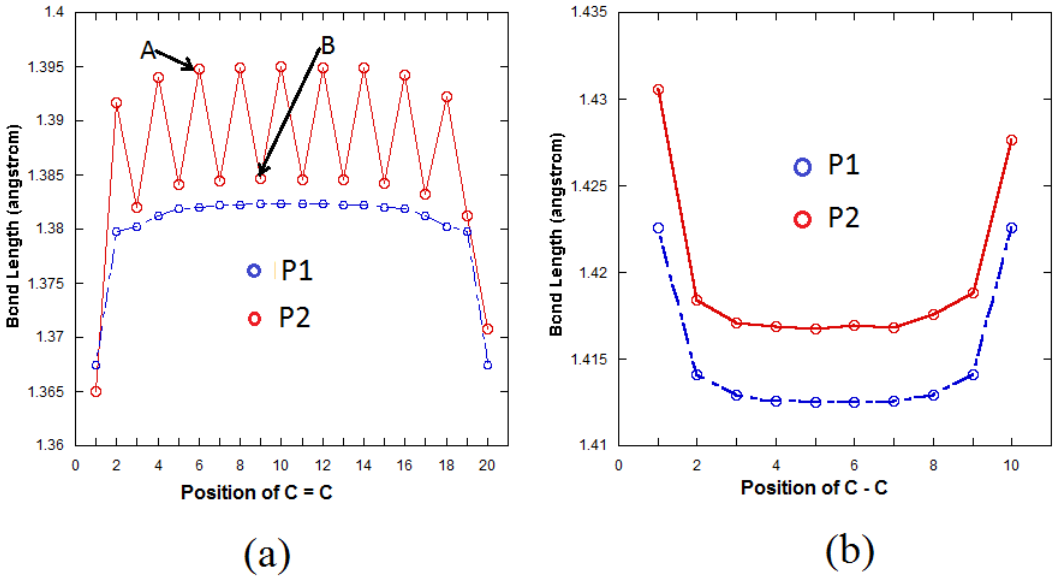

FIGURE 3.6: Bond lengths of the π bond chains of the 10-mer of P2 and P1: (a) Double-bond lengths in thiophene backbone from an end of the oligomer and (b) Single-bond lengths in thiophene backbone from an end of the oligomer.

Here, the length of thiophene double bond (A) which is near the hexyl is 1.394 Å and is larger than that of double bond (B), which is far from the hexyl (1.384 Å)[(A) and (B) are shown in Fig. 3.6(a)]. The former bond length is substantially larger than that of P1 whereas the latter bond length is close to that of thiophene. The former large bond length is expected to originate from the interaction between the hexyl and the thiophene backbone. On the other hand, the lengths of single bonds in the thiophene backbone of P2 show no oscillation at the center. The single bonds are found to be somewhat longer than those of P1, as shown in Fig. 3.6(b).

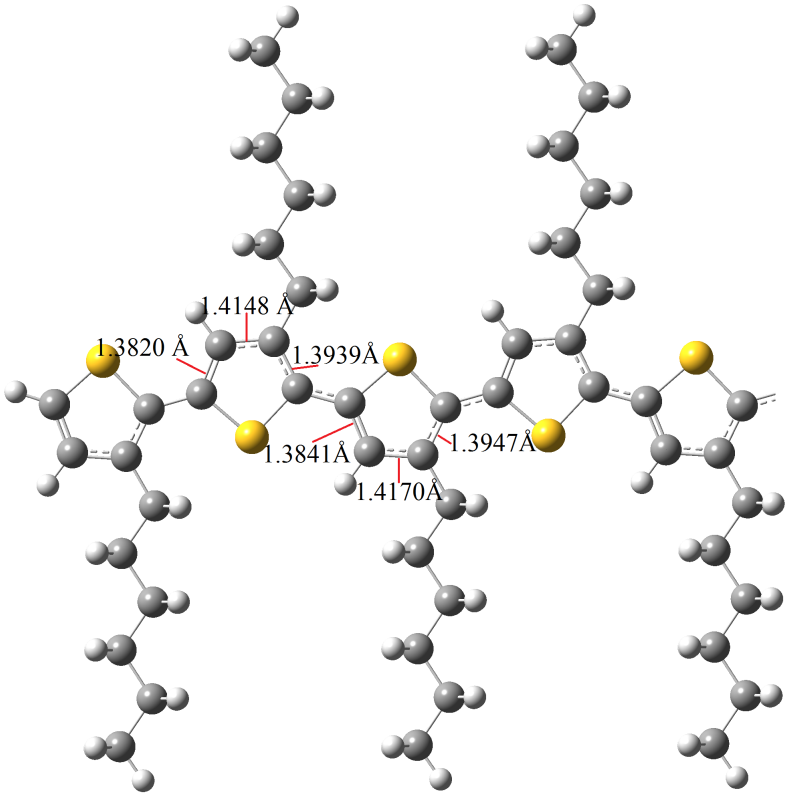

FIGURE 3.7: Molecular structure of P2.

3.2.3 Poly(2-ethenylthiophene)(P3)

We study the band gap of P3 [Fig. 1.5(c)]. We carry out hybrid-DFT calculations from the monomer to the 11-mer. Then, we estimate the band gap of the infinite-size polymer using the extrapolation scheme. The fitting is shown in Fig.3.8(a). The HOMO energy and LUMO energy of infinite-size polymer are shown in Fig.3.8(b).

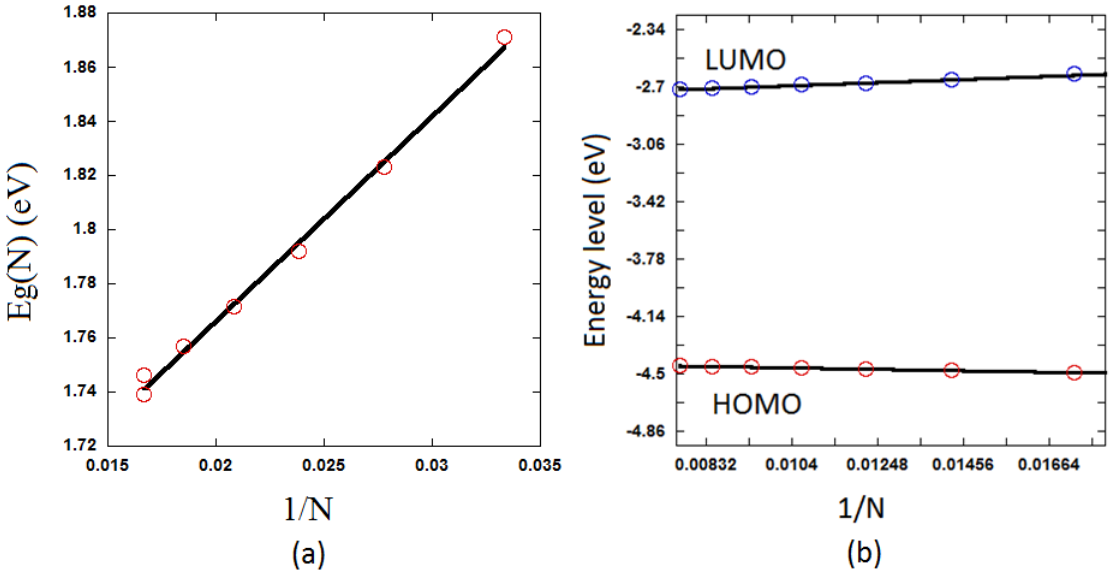

FIGURE 3.8: Calculation of P3 (a) Band gap and (b) HOMO and LUMO energy level.

The estimated band gap of P2 is 1.61 eV. The calculated energy of the HOMO in the infinite-size polymer is 0.11 eV higher than that in P1, and the energy of the LUMO in the infinite-size polymer is 0.20 eV lower than that of P1. As a result, the band gap of P3 is 0.31 eV lower than that in P1, as shown in Table 3.1.

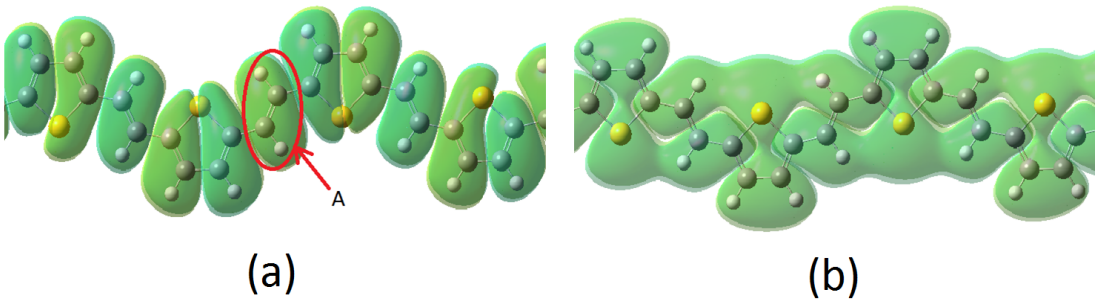

FIGURE 3.9: P3 wavefunction. The isovalue is 0.002 atomic unit: (a) HOMO wavefunction and (b) LUMO wavefunction.

The HOMO has amplitudes in the ethenyl part [which is indicated by A in Fig. 3.9(a)] as well as the thiophene part. These results indicate that both the thiophene and ethenyl parts form the π bond network, i.e., the bond alternating chain consists of the thiophene and ethenyl parts. The HOMO has the bonding and antibonding phases in the single-bond and double-bond regions, respectively, and vice versa in the case of the LUMO [Fig. 3.9(b)]. Because of the insertion of ethenyl, the π bond network of this system is quite different from that of thiophene. This difference is expected to be the reason for the low band gap of the present system.

In the case of P1, the length of the single bond [which is indicated by A in Fig. 3.10] is 1.414 Å and the length of the double bond [which is indicated by B in Fig. 2.1] is 1.381 Å. On the other hand, in poly(2-ethenylthiophene), the corresponding bond lengths are 1.407 Å and 1.389 Å, respectively, as shown in Fig. 3.11. Therefore, the bond alternation becomes weak, which contributes to the lowering of the band gap of P3, as shown in Fig. 3.11.

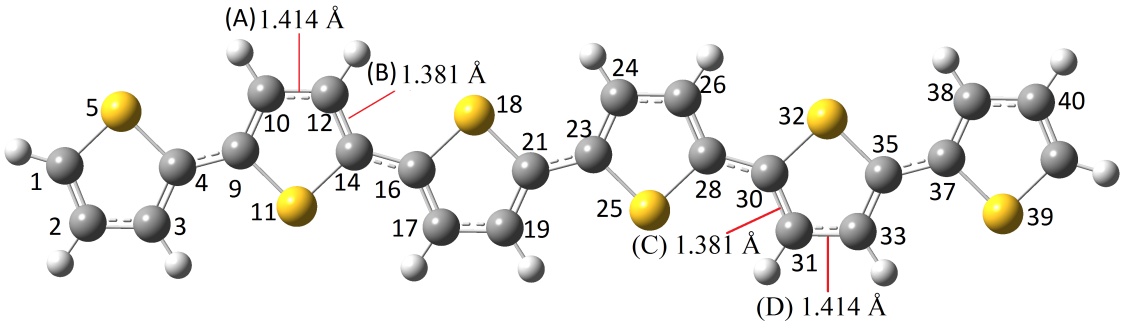

FIGURE 3.10: Molecular structure of P1.

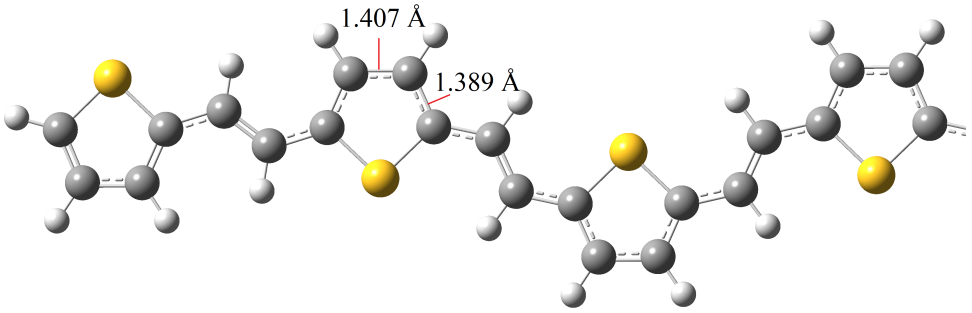

FIGURE 3.11: Molecular structure of P3.

Fig.3.12 (a) shows the weak bond alternation affects to the bond lengths with 10-mer thiophene. We find that the lengths of double bonds in the thiophene backbone of P3 is longer at the center than that of P1. On the other hand, the lengths of single bonds in the thiophene backbone of P3 show shorter at the center than that of P1 as shown in Fig.3.12(b). Therefore, the weak bond alternation contributes to the band gap decreases.

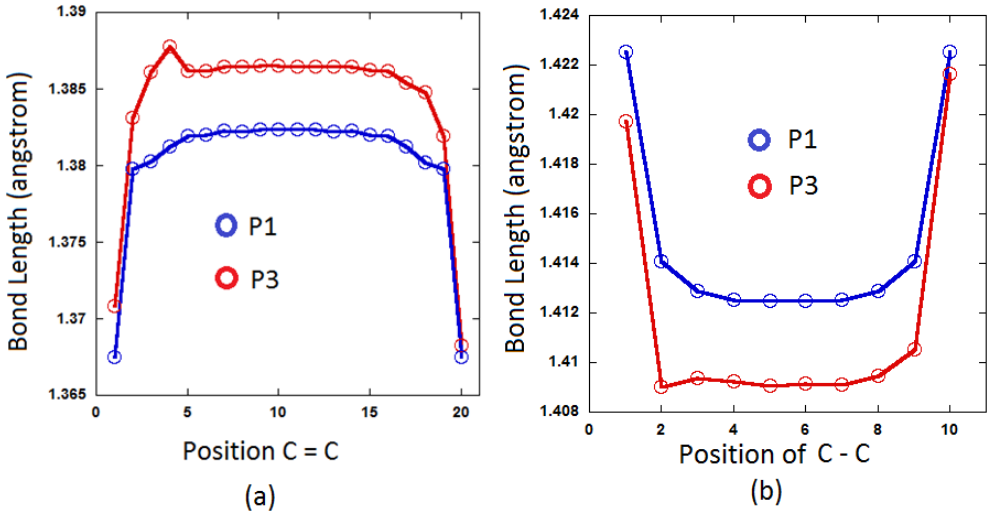

FIGURE 3.12: Bond length of P1 and P3 in 10 mer of thiophene. (a) Double bond length, (b) Single bond length.

3.2.4 PITN (P4)

P4 consists of thiophene and a benzene ring, as shown in Fig. 1.5(d). We carry out hybrid-DFT calculations from the monomer to the 15-mer. Next, we estimate the band gap of the infinite-length polymer using the extrapolation scheme. Fig. 3.13(a) shows the HOMO-LUMO gap values which are fitted well to find out the infinite band gap. The HOMO energy and LUMO energy of infinite-size polymer are also fitted appropriately as shown in Fig. 3.13(b).

The estimated band gap of PITN is 1.1 eV, which is consistent with the experimental value (1.1 eV)[3]. The calculated energy of the HOMO of PITN is 0.50 eV higher than that of polythiophene, and the energy of the LUMO of PITN is 0.32 eV lower than that of polythiophene. As a result, the band gap of PITN is 0.82 eV lower than that of polythiophene, as shown in Table 3.1.

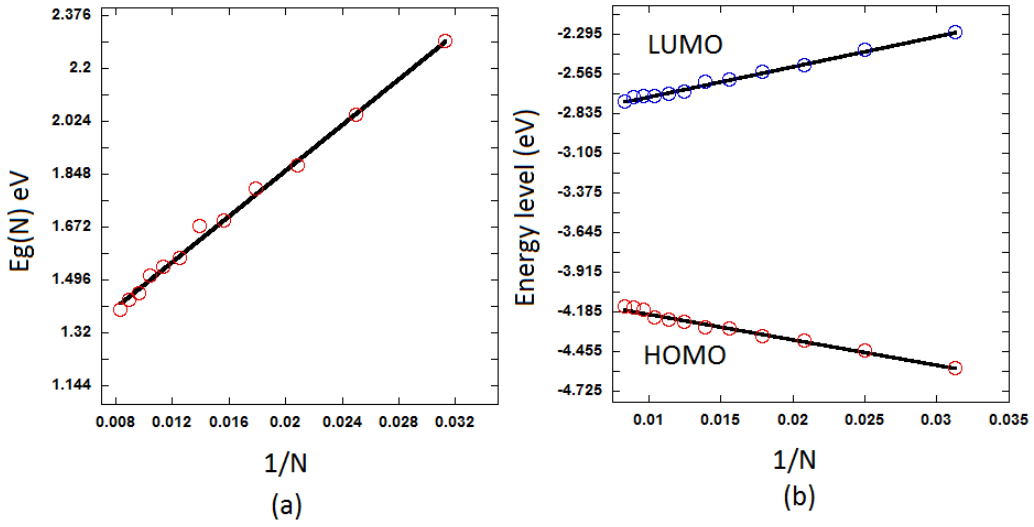

FIGURE 3.13: Calculation of P4 oligomers (a) Band gap and (b) HOMO and LUMO energy level.

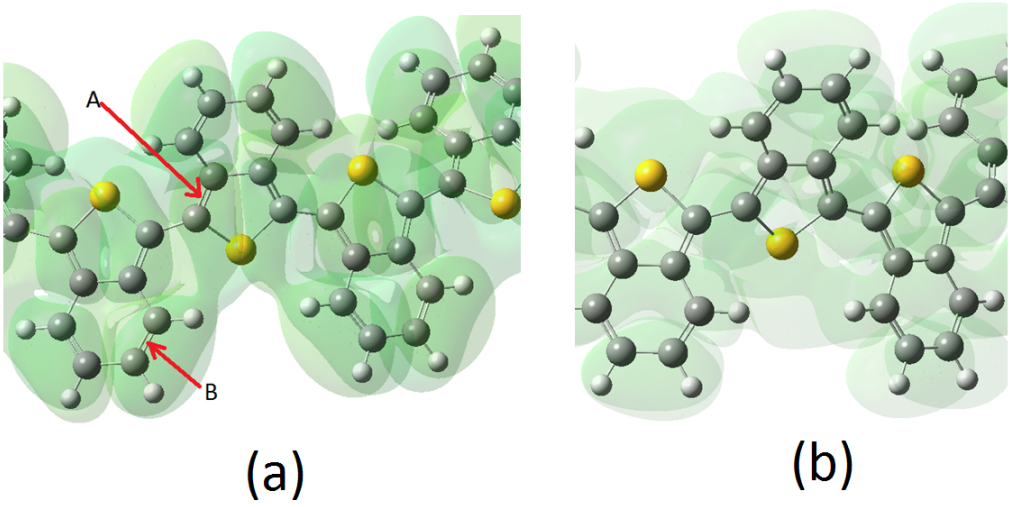

FIGURE 3.14: P4 wavefunction. The isovalue is 0.002 atomic unit: (a) HOMO wavefunction and (b) LUMO wavefunction.

The HOMO and LUMO have significant amplitudes not only in thiophene but also in the benzene ring. The amplitudes of the HOMO [Fig. 3.14(a)] and LUMO [Fig. 3.14(b)] are large in both the benzene ring and thiophene part. These results indicate that the π bond network is not restricted within the chain and is extended to the benzene ring. This extension of the π bond network is the origin of the low band gap of this polymer. Indeed, the HOMO and LUMO also have large amplitudes in the benzene ring and thiophene in the case of the monomer, and as a result, the HOMO-LUMO gap of the monomer (4.01 eV) is lower than that of the thiophene monomer (6.12 eV), as shown in Table 3.2.

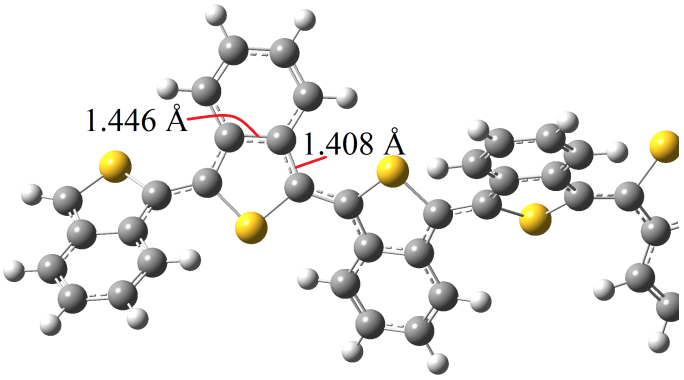

FIGURE 3.15: Molecular structure of P4.

As shown in Fig. 3.15, the geometry of the PITN is nonplanar. This is due to the fact that the double bond in the thiophene backbone of P4 (1.408 Å) is longer than that of P1 (1.381 Å) as shown in Fig. 3.10; i.e., the property of the double bond is weak in P4. Although this system is nonplanar, the HOMO and LUMO are delocalized in the polymer.

Fig. 3.16 (a) shows that the present polymer (P4) has longer bond length than the polythiophene (P1).

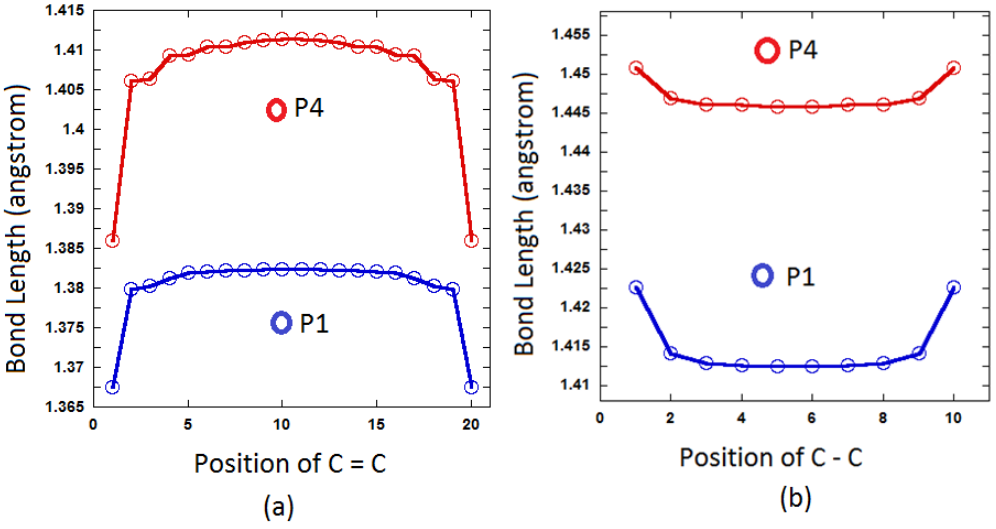

FIGURE 3.16: Bond length of P1 and P4 in 10 mer of thiophene. (a) Double bond length, (b) Single bond length.

3.2.5 Poly(2-ethenyl-3-hexylthiophene)(P5)

P5 consists of 3-hexylthiophene and ethenyl, as shown in Fig. 1.5(e). There is no experimental band gap data for this P5; therefore, we predict the band gap of this system. We carry out hybrid-DFT calculations up to the 17-mer. Then, we estimate the band gap of the infinite-length polymer using the extrapolation scheme. Fig. 3.17(a) shows the HOMO-LUMO gap values which are fitted well to find out the infinite band gap. The HOMO energy level and LUMO energy level of infinite-size polymer are also fitted appropriately as shown in Fig. 3.17(b).

The estimated band gap of P4 is 1.39 eV. Therefore, the band gap of P4 is 0.22 eV lower than that of P2. We evaluate the energies of the HOMO and LUMO in this polymer, as shown in Table 3.1. The energy of the HOMO in this polymer is 0.33 eV higher than that of P2, and the energy of the LUMO is 0.11 eV higher than that of P2. As a result, the band gap of P4 is 0.22 eV lower than that of P2, as shown in Table 3.1.

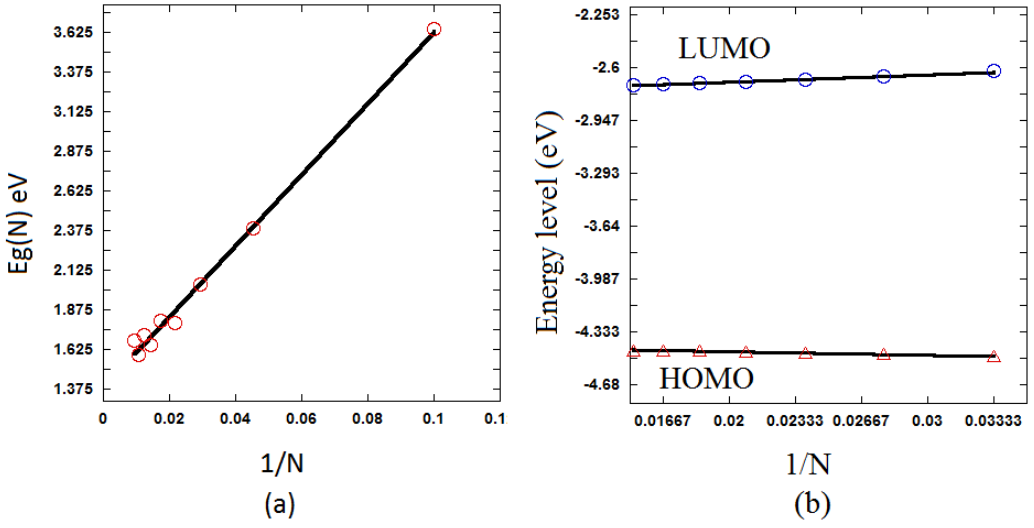

FIGURE 3.17: Calculation of P5 oligomers (a) Band gap and (b) HOMO and LUMO energy level.

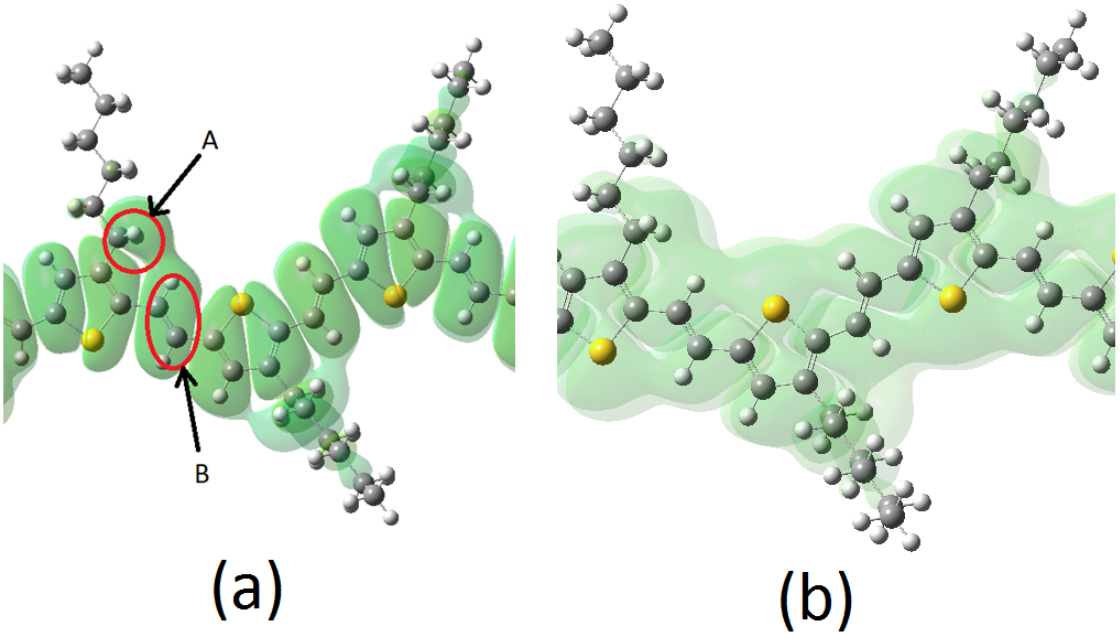

FIGURE 3.18: P5 wavefunction. The isovalue is 0.002 atomic unit: (a) HOMO wavefunction and (b) LUMO wavefunction.

The above-mentioned low band gap of this system is expected to originate from the interaction between the hexyl of the thiophene backbone [which is indicated by A in Fig. 3.18(a)] and the double bond of the ethenyl part [which is indicated by B in Fig. 3.18(a)]. This interaction leads to the fact that the large increase in HOMO energy since the HOMO has the bonding phase for the double bond in the conjugated chain [Fig. 3.18(a)]. The effect of the interaction on the LUMO is weak, as Fig. 3.18(a) shows, which leads to a small increase in LUMO energy.

Although the band gap of P5 is lower than that of P3, the HOMO-LUMO gap of the monomer of P5 (4.73 eV) is very similar to that of P3 (4.74 eV) (Table 3.2). This similarity in energy is due to the fact that there is no interaction between hexyl and the double bond in the ethenyl part in the case of the monomer of P5.

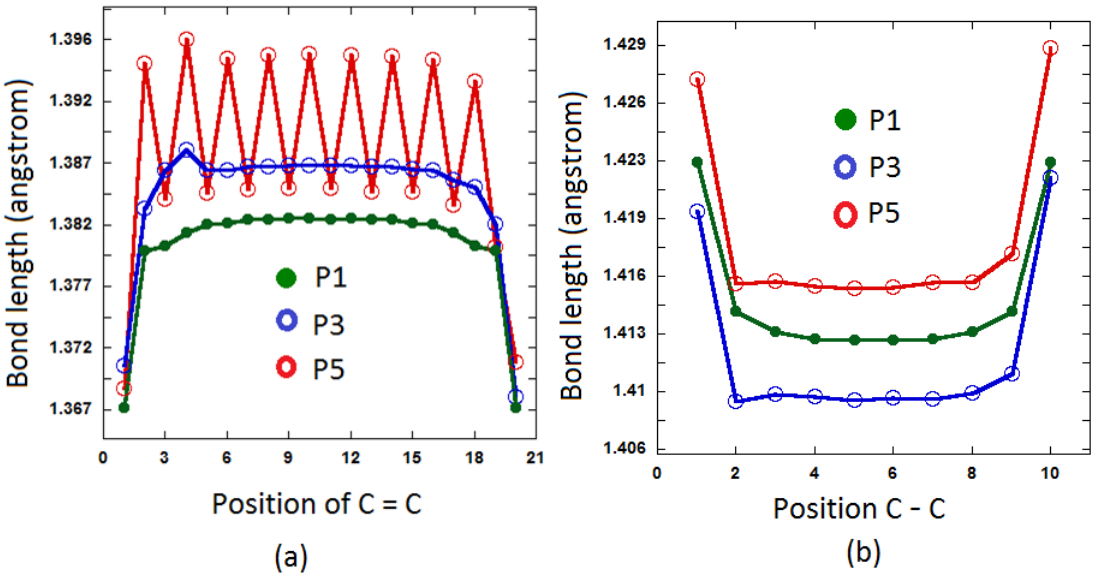

FIGURE 3.19: Bond length of P1, P3 and P5 in 10 mer of thiophene. (a) Double bond length, (b) Single bond length.

The interaction between hexyl of the thiophene backbone and the double bond of the ethenyl part affects to the bond lengths. We show the results for the 10-mer in Fig. 3.19(a). We find that the lengths of the double bonds in the thiophene backbone of P5 osccilate at the center. The double bond of P5 is longer than those of P1. However, some of the double bond of P5 are slightly longer than those of P3. On the other hand, the single bond of P5 is the longest compare to those of P1 and P3 as shown in Fig.3.19(b). Due to the interaction of the double bond and hexyl, the molecular structure of P5 is not as planar as P2 as shown in Fig. 3.20, especially in the hexyl tails.

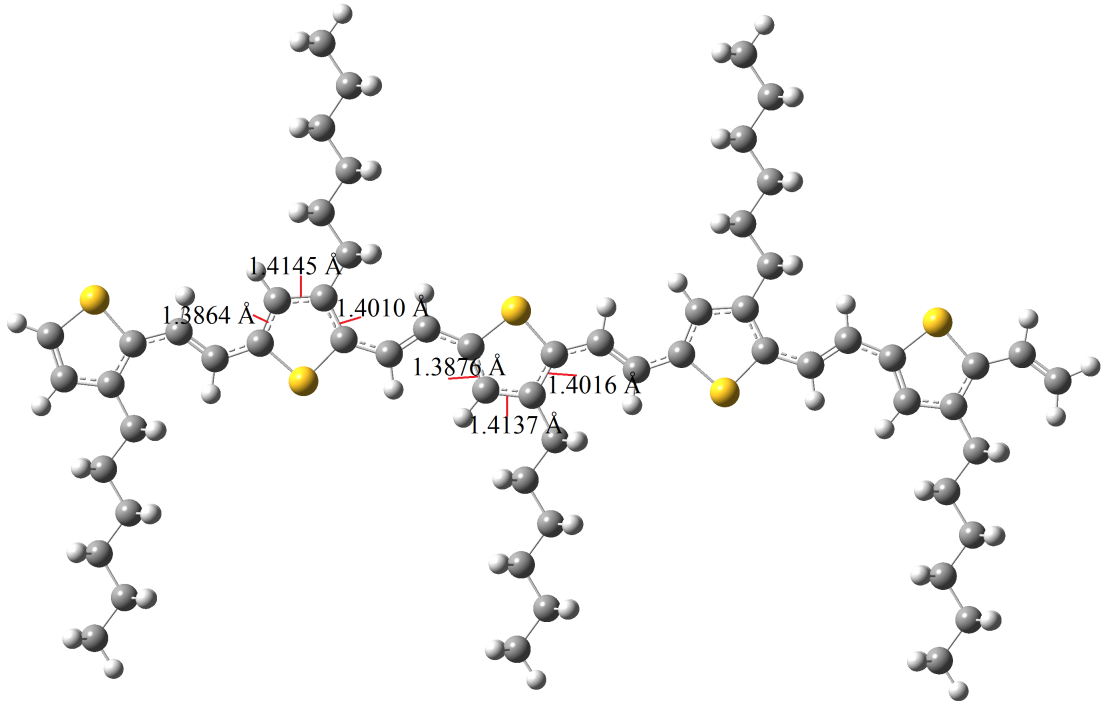

FIGURE 3.20: Molecular structure of P5.

3.3 Discussion

3.3.1 Comparison Between Results of Present and Past Calculations

We use the extrapolation scheme to estimate the band gaps of infinite-length polymers. The R^2 value of all polymers are close to 1, as shown in Table 3.1, which indicates that fitting to Eq. (2.31) is successful. The calculated band gaps are close to the experimental values, as shown in Table 3.1: The differences between the band gaps obtained theoretically and experimentally are 0.1 - 0.2 eV. Therefore, the present calculation scheme, in which the extrapolation scheme and hybrid-DFT [B3LYP/6-31G(d,p)] are used, is reliable for predicting band gaps.

The band gaps of P1 have been calculated using the extrapolation scheme and hybrid-DFT.[3, 23, 30–33] First, Salzner et al.[32] used the B3P86/CEP-31G* method and obtained a band gap value of 2.30 eV. Later, Yang et al.[23] optimized the geometry by the semiempirical (PM3) method and estimated the band gap using B3LYP. They obtained a band gap value of 1.93 eV. Zade and Bendikov[33] used the B3LYP/6-31G(d) method and obtained a band gap value of 1.81 eV. They also use the periodic boundary condition instead of the extrapolation method and obtained a band gap value of 2.06 eV. Torras et al.[31] used the B3LYP/6-31G(d) method and obtained a band gap value of 1.88 eV. As mentioned above, the estimated band gaps in past studies are 1.81 - 2.30 eV and are comparable to the present value (1.92 eV).

Yang et al.[3, 23] also estimated the band gaps of P3 and P4 to be 1.52 and 1.44 eV, respectively. These values are close to the present values (1.61 and 1.1 eV). Therefore, the present band gaps are comparable to those of past studies.[3, 23, 30–33]

3.3.2 Mechanism of Band Gap Decreases

Our finding of the decrease in band gap by modifying polythiophene indicates that the band gap of polythiophene can be suitably modified using polythiophene derivatives. Therefore, a theoretical design based on first-principles calculations is important. We discuss the mechanisms underlying the decrease in the band gaps in thiophene derivatives in previous sections. Here, we summarize the mechanisms.

(A) *Hexyl effect*

The calculated band gap of P2 is 0.11 eV lower than that of P1 and the band gap of P5 is 0.22 eV lower than that of P3. The decreases in the band gaps in the above-mentioned two polymers cases are due to the hexyl effect: there is interaction between the hexyl and the double bond in the conjugated chain as mentioned in Sects. *3.2.2* and *3.2.5*. The decrease (0.22 eV) in the band gap of P5 is larger than the decrease (0.11 eV) that of P2. This difference is expected to originate from the fact that the ethenyl double bond and the

thiophene double bond are affected by the hexyl in the former and later cases, respectively.

(B) *Ethenyl effect*

The band gap of P3 is 0.31 eV lower than that of P1. The difference in band gap between these two polymers is due to the difference between the π bond chain in the two systems: the conjugated chain consists of thiophene and ethenyl in the case of P3 and the chain consists of only thiophene in the case of P1. The weak bond alternation in P3 contributes to the decreases in band gap.

(C) *Extension of the π bond network*

The band gap of P4 is 0.82 eV lower than that of P1. In the case of P4, its HOMO [Fig. 3.14(e)] and LUMO [Fig. 3.14(e)] have amplitudes not only in thiophene but also in the benzene ring. This extension of the π bond network in P4 is the origin of the decreases in band gap.

As mentioned above, we discuss the three mechanisms underlying the band gap decreases in polythiophene derivative. These findings are helpful in the design of new derivatives having low band gaps. Actually, we predict that P5 has a low band gap (1.39 eV) due to the ethenyl and hexyl effects.

Chapter 4

Summary

4.1 Conclusion

We successfully calculate the band gap of polythiophene derivatives. We have carried out hybrid-DFT calculations for finite-size of polythiophene derivatives and estimate the band gaps of the infinite-length of polythiophene derivatives using an extrapolation scheme. The calculated band gaps of polythiophene (P1), P3HT (P2), poly(2-ethenylthiophene) (P3), and PITN (P4) are close to the experimental values. The difference of the present band gap calculation and experiment values are quite small , which is 0.1 - 0.2 eV. Therefore, the present theoretical method is found to be reliable. We also predict the band gaps of poly(2-ethenyl-3-hexylthiophene) (P5). The calculated band gaps of polythiophene derivatives studied in this paper are 1.10 - 1.81 eV; therefore, we have demonstrated that the band gaps can be controlled using suitable of polythiophene derivatives.

We clarify the mechanisms of the band gap decreases by analyzing the HOMO and LUMO as summarized in Sect. *3.3.2*. These findings are expected to be useful for band gap design. In particular, we find that the attachment of the hexyl decreases the band gap. With the correspond to this mechanism, we design poly(2-ethenyl-3-hexylthiophene) (P5). We estimate that the band gap of poly(2-ethenyl-3-hexylthiophene) (P5) has low band gap (1.39 eV).

4.2 Future Scope

In this study, we successfully predict the band gaps of polythiophene derivatives. We also clarify the mechanism the decreases of band gaps. Therefore, the low band gap of conjugated polymers can be designed.

However, for OSC besides the low band gap of conjugated polymers, we also need to achieve the low HOMO energy level. The HOMO energy level is associated to V_{oc} as shown in Eq. 1.2. The V_{oc} contributes to charge transfer. Therefore, to control the HOMO energy level, we need to design a push and pull units that allow internal charge transfer process along the conjugated chain.[34] These push pull units can be designed through the donor-acceptor(D/A) copolymers. D/A conjugated polymers consist of electron rich conjugated polymers and electron acceptor conjugated polymers as acceptors [Fig.4.1].

For furhter study, based on the band gap calculations and the mechanism of band gap decreases in polythiophene derivatives, we would like to design low band gaps polymers and the low HOMO energy level using combination of donor/acceptor (D/A) copolymer. These D/A copolymer gives future hope to control the band gap of conjugated polymers, and finally we can find the suitable conjugated polymers for OSC application.

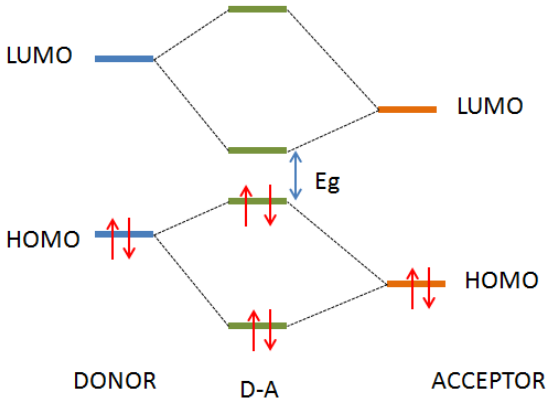

FIGURE 4.1: The band gap scheme of donor-acceptor copolymer.

Bibliography

[1] T. A. Skotheim, R. Lelsenbaumer, and J. R. Reynolds, *Handbook of Conducting Polymers*, (Marcel Dekker, New York, 1998) 3th ed., p. 13-3.

[2] H. S. Nalwa, *Handbook of Organic Conductive Molecules and Polymers*, (Wiley, Chichester, UK, 1997) Vol. 3, p. 87.

[3] I. F. Perepichka and D. F. Perepichka, *Handbook of Thiophene-based Materials*, (Wiley, Chichester, U. K., 2009) 1st ed., p. 366.

[4] H. S. Nalwa, *Handbook of Advanced Electronic and Photonic Materials and Devices*, (Academic Press, San Diego, CA , 2001) Vol. 8, p. 266.

[5] N. S. Sariciftci, D. Braun, C. Zhang, V. I. Srdanov, A. J. Heeger, G. Stucky and F. Wudl, Appl. Phys. Lett. **62**, 585 (1993).

[6] C. J. Brabec, N. S. Sariciftci, and J. C. Hummelen, Adv. Func. Mater, **11**, 1 (2001).

[7] H. Hoppe and N.S. Sariciftci, J. Mater. Ress., **19**, 1924 (2004).

[8] S. Gunes, H. Neugebauer, and N. S. Sariciftci, Chem. Rev., **107**, 1324 2007.

[9] R. Kroon, M.Lenes, J.C. Hummelen, P. W. M. Blom and B.D. Boer, Polymer Reviews, **48**, 531 (2008).

[10] M. A. Green, K. Emery, Y. Hishikawa, W. Warta and E. D. Dunlop, Prog. Photovolt: Res. Appl., **22**, 1 (2014).

[11] V. I. Arkhipov, P. Heremans and H. Bassler, Appl. Phys. Lett., **82**, 4605 (2003).

[12] X. Y. Zhu, Q. Yang, and M. Muntwiller, Acc. Chem. Res., **42**, 1779 (2009).

[13] R.M. Martin,*Electronic Structure Basic Theory and Practical Methods*, (Cambridge University Press, Cambridge, UK, 2004) 1st ed., p. 53, 119, 152.

[14] I.Y. Zhang, J. Wu and X. Xu, Chem. Commun.,**46**, 3057 (2010).

[15] W. Kohn, A.D. Becke and R.G. Parr, J. Phys. Chem., **100**, 12974 (1996).

[16] J. Paier, M. Marsman and G. Kresse, J. Chem. Phys, **127**, 024103 (2007)

[17] I. Y. Zhang, J. Wu and X. Xu, Chem. Commun., **46**, 3057 (2010).

[18] F. Jensen, *Introduction to Computational Chemistry*, (Wiley, UK, 2001) 1st ed., p.150.

[19] J. S. Binkley, J. A. Pople, and W. J. Hehre, J. Am. Chem. Soc, **102**, 939 (1980).

[20] G. Horowitz, B. Bachet, A. Yassar, P. Lang, F. Demanze, J. L. Fave, and F. Garnier, Chem. Mater. **7**, 1337 (1995).

[21] Gaussian 03, Revision C. 02, Gaussian, Inc., Wallingford, CT, 2004.

[22] T. C. Chung, J. H. Kaufman, A. J. Heegar, F. Wudl, Phys.Rev. B **30**, 702 (1984).

[23] S. Yang, P. Olishevski, and M. Kertesz, Synth. Met. **141**, 171 (2004).

[24] J. Roncali, Macromol. Rapid Commun. **28**, 1761 (2007).

[25] M. Kertezs and Y. S. Lee, J. Phys. Chem. **91**, 2690 (1987).

[26] W. Tang, L. Ke, L. Tan, T. Lin, T. Kietzke and Z. K. Chen, Macromolecules **40**, 6164 (2007).

[27] L. Zou, Y. Fu, X. Yan, X. Chen and J. Qin, J. Polym.Sci. Part A **46**, 702 (2008).

[28] J. Roncali, Chem. Rev. **97**, 173 (1997).

[29] A. D. Becke, J. Chem. Phys. **98**, 5648 (1993).

[30] S. S. Zade, N. Zamoshchik and M. Bendikov, Acc. Chem. Res. **44**, 14 (2011).

[31] J. Torras, J. Casanovas and C. Aleman, J. Phys. Chem. A **116**, 7571 (2012).

[32] U. Salzner, P. G. Pickup and R. A. Porier, J. Phys. Chem. A, **102**, 2572 (1998).

[33] S. S. Zade and M. Bendikov, Org. Lett. **8**, 5243 (2006).

[34] I. McCulloch, R. S. Ashraf, L. Biniek, H. Bronstein, C. Combe, J.E. Donaghey, D.I.James, C.B. Nielsen, B.C. Schroeder, and W. Zhang, Account Chem Res., **45**, 714 (2014).